REPUBLIC OF TÜRKİYE

ALTINBAŞ UNIVERSITY

Institute of Graduate Studies

Electrical and Computer Engineering

AGE AND GENDER CLASSIFICATION IN EEG SIGNALS USING DEEP LEARNING

Khalid Tawfiq Abdulalbaqi AL-DIWAN

Master's Thesis

Supervisor

Prof. Dr. Galip Cansever

Istanbul, 2023

AGE AND GENDER CLASSIFICATION IN EEG SIGNALS USING DEEP LEARNING

Khalid Tawfiq Abdulalbaqi AL-DIWAN

Electrical and Computer Engineering

Master's Thesis

ALTINBAŞ UNIVERSITY

2023

The thesis titled AGE AND GENDER CLASSIFICATION IN EEG SIGNALS USING DEEP LEARNING prepared by KHALID TAWFIQ ABDULALBAQI AL-DIWAN and submitted on x/x/2023 has been **accepted unanimously** for the degree of Master of Science in Electrical and Computer Engineering.

Prof. Dr. Galip Cansever

Supervisor

Thesis Defense Committee Members:

Prof. Dr. Galip Cansever	Department, University	____________________
Academic Title - First/Last Name	Department, University	____________________
Academic Title - First/Last Name	Department, University	____________________

I hereby declare that this thesis meets all format and submission requirements of a Master's thesis.

Submission date of the thesis to Institute of Graduate Studies: ___/___/___

I hereby declare that all information and data presented in this graduation project has been obtained in full accordance with academic rules and ethical conduct. I also declare all unoriginal materials and conclusions have been cited in the text and all references mentioned in the Reference List have been cited in the text, and vice versa as required by the abovementioned rules and conduct.

Khalid Tawfiq Abdulalbaqi AL-DIWAN

Signature

ACKNOWLEDGEMENTS

Thank you to my supervisor, Prof. Dr Galip Cansever for providing guidance and feedback throughout this project. Thanks also to my wife Anna, for putting up with me being sat in the office for hours on end, and for providing guidance and a sounding board when required

ABSTRACT

AGE AND GENDER CLASSIFICATION IN EEG SIGNALS USING DEEP LEARNING

AL-DIWAN, Khalid Tawfiq Abdulalbaqi

M.Sc., Electrical and Computer Engineering, Altınbaş University,

Supervisor: Prof. Dr. Galip Cansever

Date: August / 2023

Pages: 87

The most recent advancements in this field have made it possible for a vast array of BCI-based applications to be created, which has led to an explosion in the number of such applications. In this study, we suggest a novel application of BCI, which entails estimating a person's age and gender based on the analysis of their electroencephalogram (EEG). The brainwave activity of sixty distinct individuals, both male and female, was recorded while they were sleeping peacefully with their eyes closed by using equipment that is considered to be standard EEG recording gear. A hybrid learning architecture was constructed with the aid of a deep CNN network so that this analysis could be carried out.

Keywords: EGG, CNN, DNN, MRI, RNN.

TABLE OF CONTENTS

Pages

LIST OF TABLES

Pages

LIST OF FIGURES

Pages

ABBREVIATIONS

ML	:	Machine Learning
DL	:	Deep Learning
MRI	:	Magnetic Resonance Imaging
CNN	:	Convolutional Neural Networks
DNN	:	Deep Neural Network
RNN	:	Recurrent Neural Network
EEG	:	Electroence Phalography

1. INTRODUCTION

1.1 BACKGROUND

The developmental age prediction is a statistic that is one that may be utilized for the purpose of assessing whether or not this should be done. The hypothesis that neuroimaging methods, and more especially the data received from MRIs, may be able to properly forecast a person's chronological age has been supported by a substantial body of research, lending validity to the theory. Because it is still a relatively novel method, estimating a person's age from their EEG data and doing so via the use of machine learning, there is a paucity of study conducted in this area. In recent years, it has been shown that EEG data recordings may be used to estimate a human's developmental age using normal machine learning methodologies. This discovery came about as a result of studies conducted in the United States and Europe. The patterns of electrical activity in the brain were analyzed, which allowed for the successful completion of this task. This discovery was discovered quite recently, over the course of a number of years' time. When doing study of the sort that this one undertakes, which includes the evaluation of MRI and EEG data, it is not unusual to discover that an individual's actual age is considerably different from the age that is projected for them based on the brain scans that were performed on them.

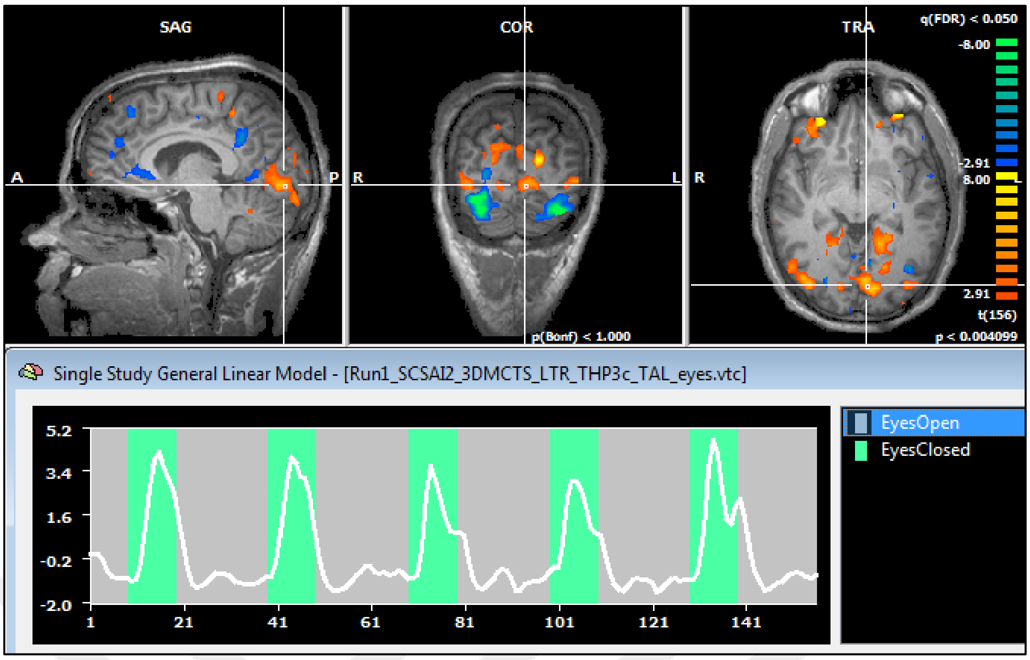

Figure 1.1: EEG and MRI Data Corelation.

It has been proposed that the magnitude of this gap might serve as a biomarker for determining how far advanced in its developmental process a person's brain is at a certain moment in time. Although a huge number of investigations have been carried out on the topic of age prediction via the examination of EEG data, only a small part of these research has concentrated on the use of deep learning algorithms. In recent years, deep learning has been shown to be successful in a range of applications, including image classification and natural language processing, to mention just two of those domains. Deep learning has also been shown to be useful in a number of other applications.

To achieve this goal, one of the objectives of this research is to determine whether or not deep learning can improve the accuracy of developmental age prediction by making use of an EEG data collection, and if so, to what degree this enhancement can be achieved. This will be accomplished by determining whether or not deep learning can improve the accuracy of developmental age prediction by using an EEG data collection. The information that we used came from research that can be found here. If one of these methods were capable of accurately estimating a subject's developmental age, it would be evidence that deep learning algorithms are capable of consistently identifying characteristics of subjects. This would be significant because it would demonstrate that deep learning algorithms can be applied to a wide variety of domains. Electroencephalograms could be able to identify novel traits or biomarkers in this particular context.

1.2 PROBLEM STATEMENT

This study creates predictions about ages by use regression rather than classification, which is another another way in which it is unique from studies that have been conducted before (using deep learning). First, in order to employ deep learning, Kaushik and his colleagues divide their subjects into groups according to their ages, and then they use these age groups as labels for the purpose of training their model. This process is repeated many times.

In order to check whether or not the model is accurate, the data that has been gathered but has not yet been analyzed is split up into one of these categories and then analyzed. On the other hand, the feasibility of these models is highly reliant on the age group range that is selected as the focus of their attention. It is not at all difficult to achieve great levels of accuracy when the groupings that are being fired at have capabilities that span a large range. This paves the way for two new applications of regression, the first of which is determining whether there is a significant difference in brain age, and the second of which is improving one's understanding of the model by comparing the projected age to the actual age of the subject being studied. Both of these applications can be accomplished by using the information provided by the regression. Because of the fact that this door has been opened, both of these applications are now within reach of being implemented. As a result of this, rather than providing a ballpark figure for the subject's age, we will use regression to determine the subject's true age in order to avoid any errors (in months).

Because of the complexity of these models, which require a huge number of factors and layers, they are frequently referred to as "black boxes." This is because black boxes conceal information rather than revealing it. The ability of a model to accurately forecast future occurrences comes at the expense of the model's ability to provide an explanation for those events. Researchers that are working in the subject of explainable artificial intelligence have made several efforts over the course of the last few years to achieve knowledge of these incomprehensible systems. Before we could use deep learning models for medical diagnosis, we would need the ability to access tools that would allow us to analyze the level of uncertainty that would be produced by the model as well as the reasoning that would lead to the conclusion. Without these tools, we would not be able to use deep learning models for medical diagnosis. In conclusion, we have high hopes that our investigation will enlighten us on the processes that are responsible for the results that are generated by the models that we have provided. These hopes are based on the fact that we have high hopes that our investigation will enlighten us on these processes.

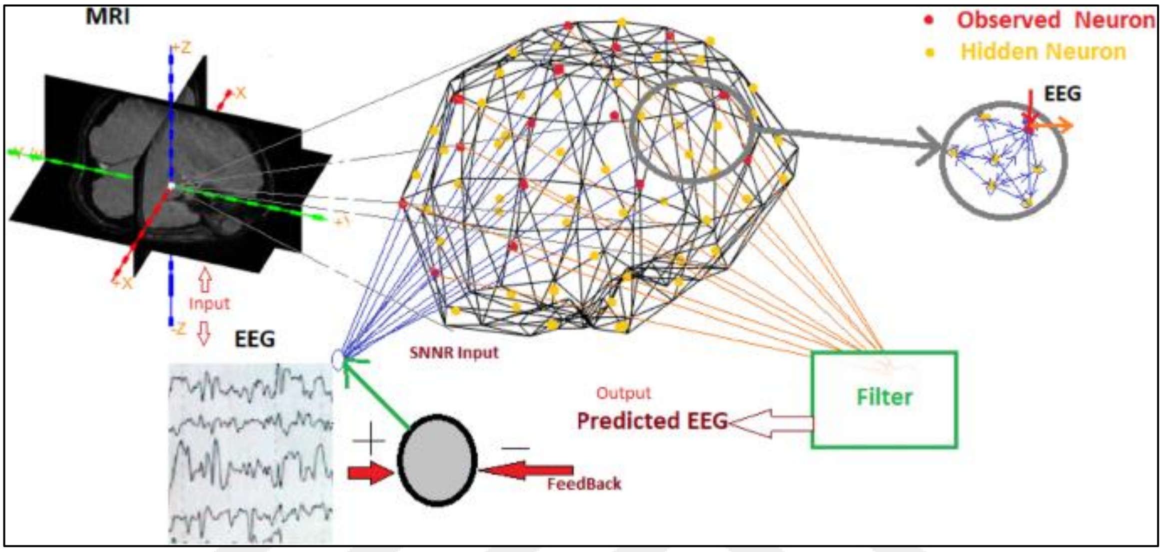

Figure 1.2: Extraction of EEG Data.

The process of validation is an essential component of not just modeling brain aging in general but also machine learning in specific. During the course of our inquiry, we make use of a data collection that comprises additional characteristics in total. During the process of validating the model, several additional characteristics could be taken into consideration.

We are able to determine whether or not there is a link between the subjects' projected developmental years and their actual ages by analyzing the quantity of language possessed by the respondents. If this turns out to be true, it lends credence to the notion that one would be able to determine the degree of brain development based on the EEG readings of a person's scalp. The capacity of the models to effectively forecast an individual's age will also be evaluated depending on whether or not the subject of interest has a documented history of dyslexia. This will be done to determine whether or not the models are accurate.

1.3 OBJECTIVES

Taking into consideration the overarching purpose of this study, the following issues were identified as particular research objectives:

i. Investigate whether or if there are discernible differences, based on statistical analysis, between the populations of young people and senior individuals.
ii. Investigate whether or if there is a linear trend that emerges as a function of the ages of the people;
iii. Investigate the possibility of developing new tools and approaches for evaluating EEG data, which may reveal changes in signal characteristics with advancing age;
iv. Apply the LDA method, also known as the Value linear discriminant analysis, to the EEG signals that were collected from the several groups that are being investigated.
v. Apply the LDA method, also known as value linear discriminant analysis, to each frequency range of the EEG signals that were collected from the groups that are being analyzed;
vi. Determine whether or not there are differences that may be considered statistically significant between the frequency ranges and the groups that are being looked at;
vii. Provide recommendations for further research that might be carried out in light of this study.

1.4 CONTRIBUTION

the present study adds by collecting control data (such as the impact of healthy aging on EEG data), which can then be compared to clinical data based on resting-state EEGs. This allows for a more in-depth analysis of both sets of data (e.g., influence of unhealthy aging to EEG data). The studies that came before lacked essential information on the several sources that were used. To the best of our knowledge, this is the first effort to offer source-level reference data by analyzing the effects of healthy aging and gender on a single dataset using EC and EO settings.

This is the scenario, to the best of our knowledge, according to the available information. We used electroencephalography, or EEG, to record the levels of brain activity that were present at rest in a total of 54 females and 48 males with normal cognitive function and ages ranging from 22 to 75 years old. The participants' ages ranged from 22 to 75 years old. Our goal was to get an understanding of the ways in which the effects of age and gender differ throughout the different regions of the brain. This work adds new evidence to the growing body of research that demonstrates the validity and reliability of using resting-state functional neuroimaging in therapeutic contexts. In this study, we also propose a speech-based approach for extracting paralinguistic properties from EEG signals that contain rich age and gender information. The goal of this technique is to improve the accuracy of the gender and age classifications that we are able to generate. The results of the tests that were conducted to evaluate and contrast the systems are also shown here.

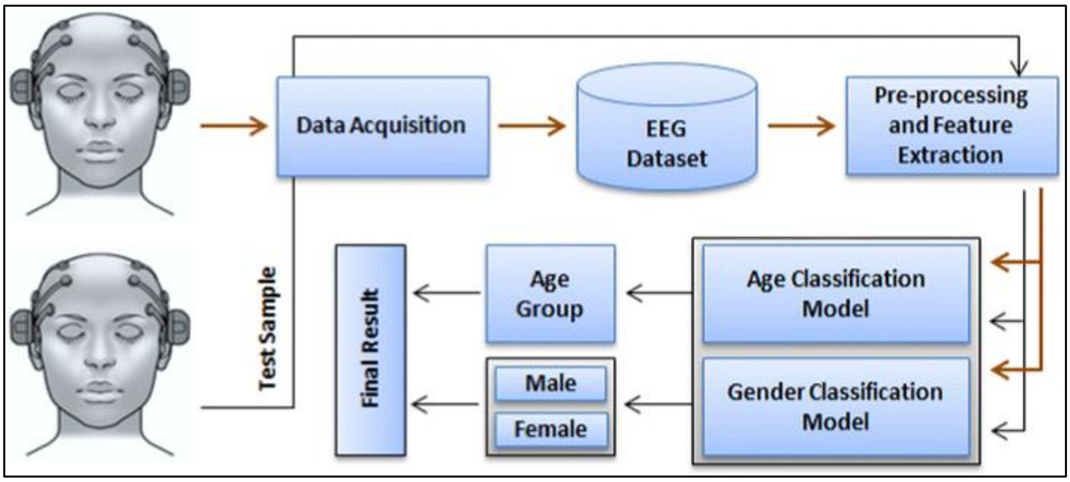

Figure 1.3: Outline of the Proposed Method.

1.5 THESIS STRUCTURE

Deep Learning and other types of neural networks used in the development of systems for recognizing patterns of EEG signals under stimulation of steady-state visual evoked potentials

In chapter 2 basic concepts on electromyography at the brain-machine interfaces are presented and the main regions of the brain are studied, the distribution of electrodes for acquisition to EEG signals and some sensory evoked potentials through extensive research on literature review.

In Chapter 3, the main characteristics of the brain-machine interfaces are described, their classification, internal structure, as well as the pre-processing of signals related to the extraction. action of characteristics of EEG signals.

In Chapter 4, the Software and Hardware used in the development of this research are presented, explaining why to compile Machine Learning or Deep Learning algorithms on a CPU and a GPU, describing the Framework used for Deep Learning.

2. LITERATURE REVIEW

2.1 INTRODUCTION

The first kind is a taxonomy that is based on medical activities (including the detection of sickness, computer-assisted diagnostics, and other similar activities) or anatomically-related application areas (i.e., brain, eyes, chest, lung, liver, kidney, heart, etc.). The compilation of research on deep learning algorithms for assessing physiological data that was done by Faust et al. [6] covers the years 2008 to 2017, and it is made up of 53 different studies that were done independently. The writer of this piece started out by introducing a large number of different deep-learning models. The auto-encoder, the deep belief network, the restricted Boltzmann machine, the generative adversarial network, and the recurrent neural network were some of the others. After that, the physiological signals were categorized into a wide variety of subgroups according to the multiple kinds of data that were employed to collect them. Within their respective areas, the medical application, the deep learning approach, the data, and the results have all been correctly identified.

The second focuses on deep learning and contains subjects such as a taxonomy of deep learning architectures (including AE, CNN, RNN, DBN, GAN, U-Net, and more), as well as a strategy for using deep learning in a medical environment. Ganapathy et al. [3] conducted a study to investigate the effectiveness of deep learning on one-dimensional biosignal data that was structured according to a taxonomy. For the purpose of this research, we gathered seventy-one articles that were published between the years of 2010 and 2017. The bulk of the information that was acquired focused on the EKG findings (ECGs). The evaluation of a variety of deep learning-based approaches to biosignal analysis was the primary aim of this study when it was first conceived. After that, it categorized deep-learning models according to where they were formed, the size of their datasets, the kind of ground-truth data they employed, as well as the frequency with which the network was directed to gain new information.

2.2 RELATED WORKS

According to Tobore et al. [7], the use of deep learning as a method for resolving issues that arise in the healthcare industry presents a number of challenges that are associated with the biological sphere. These difficulties might potentially be divided up into a few distinct groups. The use of deep learning in the medical field was demonstrated by first segmenting deep learning into a number of distinct application areas, which included biological systems, electronic health records, medical imaging, and physiological signals, amongst others. This allowed the application of deep learning to be better understood. In order to bring this discussion to a close, some potential avenues for further study were discussed and emphasized. Each of these avenues carries with it the possibility of bringing about improved health management via the use of physiological signals.

Both Chambon et al. [8] and Andreotti et al. [9] utilised the data that was collected using a variety of various polysomnography (PSG) techniques in the research that they conducted. The researchers Yildirim et al. [10] found that the improvement in quality of their study was due to the inclusion of EEG and EOG data. [Further citation is required] Electroencephalography (EEG) and magnetoencephalography were both used in the research that Croce et al. [11] conducted, and their findings were included into the study (MEG). There are a wide variety of areas in which convolutional neural networks may be used. Two examples of this kind of application are the categorization of the different stages of sleep and the differentiation between natural and artificial components. The number of distinct deep learning models that were used in order to accomplish the job of identifying the various phases of sleep over the course of the process of analyzing the data (Figure 6).

In order for individuals to have a better understanding of Chinese sign language, Yu et al. [10] developed a feature-level fusion of the two languages. To be more exact, the extracted features are a mixture of those that were developed manually and those that were learnt by a DBN. This was done in order to improve the accuracy of the results. This was done in order to ensure that the features are compatible with a wide range of different applications. This was done in order to guarantee that the results are as precise as is reasonably attainable. These two feature levels are mixed whenever data is sent into a deep belief network or a fully connected network for the purpose of training. This is handled in an automated manner. The researchers Li et al. used a Deep Neural Network (DNN) in their study [14] that comprised a stack of 2layered autoencoders in conjunction with a SoftMax classifier in order to classify the various amounts of force that a person employs while holding an object with their hands. This was done in order to classify the various amounts of force that a person employs while holding an object. Saadatnejad and colleagues [35] devised a method that enables the continuous monitoring of the categorizing of heartbeats on an ECG. Raw electrocardiogram recordings were segmented into RR interval characteristics and wavelet features by using the methodologies that were devised. The rhythm of the pulse was used as a measuring stick to evaluate how well these procedures worked. After that, the gathered attributes were put to use in the process of training two unique RNN-based models, which were then put to use in the classification procedure. After the characteristics had been obtained in their entirety, this technique was carried out. Jeon et al. [44] were able to detect premature ventricular contraction by using a modified weight and bias based on the error backpropagation technique and the QRS pattern of the electrocardiogram. This enabled them to identify the condition. This was made possible by the use of a modified weight and bias. They were able to arrive at an appropriate diagnosis of the condition as a result of this information. Because they had this knowledge, they were in a position to determine whether or not the premature contraction in the ventricle was the result of this. In other words, they were able to determine whether or not it was a direct effect of this. On the basis of ECG data, Liu et al. [59] developed a method for identifying cardiac illnesses that incorporated the use of LSTM for the goal of classification. This method was published. In order to accomplish the task of feature extraction in this method, the method of symbolic aggregate approximation, which is also referred to by its acronym SAX, was used. According to the findings of their study [46], Majidov and colleagues found that classifying the data received from EEG motor imaging was useful. [Citation needed] In addition to contrasting 100-unit-outputting convolutional, SoftMax, and fully-connected layers, they used Riemannian geometry to the process of feature extraction. By using fast Fourier transform energy maps (FFTEM) for the goal of feature extraction and convolutional neural networks (CNN) for the purpose of classification, Abbas et al. [87] were able to construct a classification model for motor pictures. The classification of the data pertaining to the motor images was finished off effectively thanks to the help of this model.

The purpose of the feature-level fusion that Yu et al. [9] developed was to help individuals have a better understanding of Chinese sign language. To be more exact, the extracted features are a mixture of those that were developed manually and those that were learnt by a DBN. This was done in order to improve the accuracy of the results. This was done in order to ensure that the features are compatible with a wide range of different applications. This was done in order to guarantee that the results are as precise as is reasonably attainable. These two feature levels are mixed whenever data is sent into a deep belief network or a fully connected network for the purpose of training. This is handled in an automated manner. Using a Deep Neural Network (DNN) that is made up of a stack of 2-layered autoencoders and a SoftMax classifier, Li et al. [14] were able to classify the different degrees of force that are delivered when a hand is gripped. [Citation needed] This DNN is used in order to identify the different degrees of force that are applied when a hand is grasped. Utilizing principal component analysis, or PCA, helps bring the total number of dimensions that may be accessed down to a more manageable level. Saadatnejad and colleagues [35] devised a method that enables the continuous monitoring of the categorizing of heartbeats on an ECG. Raw electrocardiogram recordings were segmented into RR interval characteristics and wavelet features by using the methodologies that were devised. The rhythm of the pulse was used as a measuring stick to evaluate how well these procedures worked. After that, the gathered attributes were put to use in the process of training two unique RNN-based models, which were then put to use in the classification procedure. After the characteristics had been obtained in their entirety, this technique was carried out. Jeon et al. [44] were able to detect premature ventricular contraction by using a modified weight and bias based on the error backpropagation technique and the QRS pattern of the electrocardiogram. This enabled them to identify the condition. This was made possible by the use of a modified weight and bias. They were able to arrive at an appropriate diagnosis of the condition as a result of this information. Because they had this knowledge, they were in a position to determine whether or not the premature contraction in the ventricle was the result of this. In other words, they were able to determine whether or not it was a direct effect of this. On the basis of ECG data, Liu et al. [59] developed a method for identifying cardiac illnesses that incorporated the use of LSTM for the goal of classification. This method was published. In order to accomplish the task of feature extraction in this method, the method of symbolic aggregate approximation, which is also referred to by its acronym SAX, was used. In the study that they conducted [45], Majidov and his colleagues argued that the data obtained from electroencephalogram (EEG) motor imaging have to be categorized. In addition to contrasting 100-unit-outputting convolutional, SoftMax, and fully-connected layers, they used Riemannian geometry to the process of feature extraction. The classification approach for multiclass motor imaging that was suggested by Abbas et al. [47] makes use of the Fast Fourier Transform Energy Map, which is sometimes referred to by its acronym, FFTEM. The process of extracting features from this map is under underway. The process of categorization is handled by this model via the use of convolutional neural networks. In order to diagnose brain illnesses, Golmohammadi et al. [44] used linear frequency cepstral coefficients (LFCC) for feature extraction and a mixture of hidden Markov models and a stacked denoising autoencoder (SDA) model for classification. Cepstral linear frequency coefficients are denoted by the abbreviation LFCC.

An LSTM-based model that incorporates error profile modeling was proposed by Chauhan et al. [26] as a method for collecting data from ECG abnormalities. This model was recommended as a means to collect data from ECG abnormalities. This concept was proposed as a means of gathering data from ECG anomalies that were not normal. This model would serve the purpose of a tool if it were used. After this step was finished, a number of well-known machine learning classifier models were studied, such as multilayer perception, support vector machine, and logistic regression. Yang et al. [41], who conducted their research with the assistance of the DLCCANet and TLCCANet feature extractors, were the ones that made the discovery of arrhythmia. Electrocardiograms with dual and three leads were used throughout the process of arriving at their findings and conclusions (ECGs). The DLCCANet and TLCCANet feature extractors were put to good use, and as a consequence, this objective was accomplished with flying colors. Following the recovery of the characteristics was the third stage, which was to run them through a linear support vector machine in order to classify them. This phase happened after the first step of retrieving the characteristics. The previous stage, which consisted of extracting the attributes, was followed by this one. Nguyen et al. [62] proposed a method for determining whether or not an automated external defibrillator (AED) has detected sudden cardiac arrest in a patient by using a convolutional neural network as a feature extractor (CNNE) and a boosting (BS) classifier. This method uses a convolutional neural network as a feature extractor (CNNE) and a boosting (BS) classifier. This technique makes use of a defibrillator that is automated and worn outside the body (AED). Ma et al. [31] developed a model as a possible answer to the problem of the driver being fatigued in order to solve the issue. This research makes use of principle component analysis (PCA) as well as a method to deep learning known as

PCANet in order to help feature extraction from inside the network model. Specifically, the goal was to better understand how to predict network behavior. These two approaches were both put into practice. As the last step in the process, the information will be classified utilizing SVM and KNN, respectively.

3. MATERIALS AND METHODS

3.1 THE ANATOMY OF THE BRAIN

The brain is an organ present inside the cranial cavity with an ovoid shape, with a convex supero-lateral surface and a transversely hollowed inferior surface (Figure 3.1).

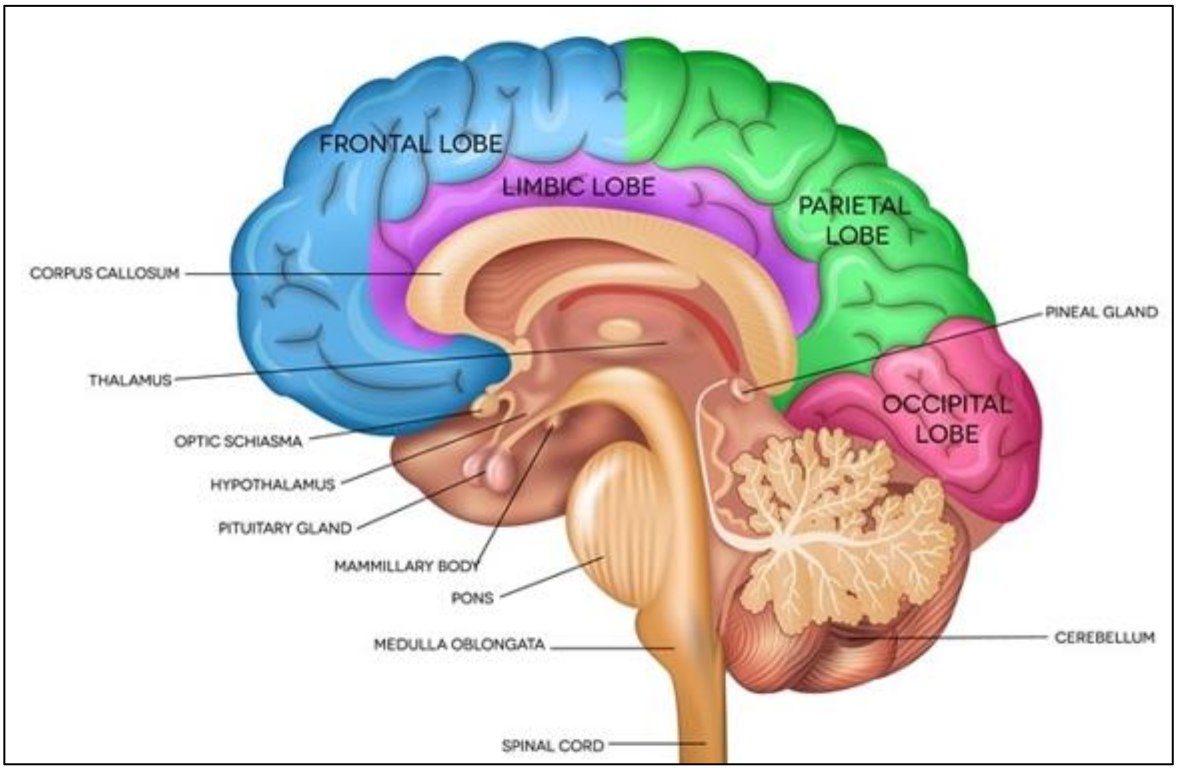

Figure 3.1: The Anatomy of the Brain.

It is wrapped in its entirety by the meninges, which guarantee the separation from the bony walls of the cranial cavity and from the cerebellum. The main building blocks of the brain are the two cerebral hemispheres (right and left) and the dienphalic region.

The two cerebral hemispheres are two anatomically distinct elements and find union in the central-lower portion of the median face through the course callosum. The gray matter and the white matter are the two substances constituting the two hemispheres. The gray matter forms the cerebral cortex, which surrounds the white matter through a neopallium. The bark has a morphology characterized by fissures and furrows; these furrows and recesses give the cortex a surface area that is twice as large and allow identification in each of the two hemispheres, lobes and convolutions. The cerebral lobes owe their name to the bones to which they correspond (frontal, parietal, temporal and occipital), to the type of conformation (libic lobe) or simply to names consolidated over time (insula lobe).

The convolutions generally take the name of the lobe to which they belong with the positional indication with respect to another descriptive element (e.g. ascending frontal or pre-Rolandic or pre-central convolution.

Within the hemispheres, the corpus callosum and the lateral ventricles are the macroscopically most relevant structures.

The corpus callosum is a laminar, transverse formation, and is formed by bundles of myelinated fibers that connect the two hemispheres together. The lateral ventricles are located under the corpus callosum; these are connected through a foramen present in each known as

"Foramen of Monro".

The amygdala, striatum, and claustrum are the three components that make up the basal ganglia, which are found in the cerebral cortex of the lower hemisphere of the brain. The hippocampus, which is also referred to as the horn of Ammon, may be found in the corpus callosum. The fornix, which is also referred to as the cerebral trigone, can also be found in the corpus callosum. The medial part of the frontal horn of the lateral ventricle, which is formed by the juxtaposition on the sagittal plane of two mainly fibrous laminae stretching between the corpus callosum and the fornix, is what forms the pellucid septum. The corpus callosum and the fornix are both located in the middle of the lateral ventricle.

The diencephalic region is located at the edge of the cavity of the third ventricle. Anteriorly it borders on the regions of the hilum and septum, on the sides with the internal capsule, caudally it continues with the midbrain: dorsally it borders on the epithalamus, ventrally on the subthalamus; It is made up mostly of gray matter. The third ventricle is a funnel-shaped cavity, in relationship, through the most sloping portion, with the pituitary; it is in communication with the lateral ventricles and with the Sylvian aqueduct in the posterior part.

The other two main formations are the optic thalamus and the hypothalamus.

The optic thalamus (with the two medial and lateral geniculate bodies), is an ovoid-shaped structure of gray matter; its rear end is characterized by a relief called pulvinar. It is covered by thin sheets of white substance which subdivide it, facilitating the topographical partition of its numerous nuclei.

The hypothalamus sits on the central portion of the base of the brain. On its ventral surface, which is related to the optic chiasm, are the mamillary bodies, the tuber cinereum and the infundibulum. In the gray matter there are numerous nuclei constituting the anatomical substrate of two neurosecretory systems, the magnocellular and the parvicellular, so called due to the dimensions of the elements that form them: the first is connected to the neurohypophysis by the hypothalamic-pituitary tract, formed by the axons of the its neurons; the second is connected to the adenohypophysis by a vascular structure, the venules of the hypothalamic-pituitary portal system, a direct continuation of the sinusoidal capillaries which permeate the tuberin region and the base of the infundibulum.

3.2 THE PHYSIOLOGY OF THE BRAIN

The brain plays the leading role in the reception, transmission, processing of different information and in the organization of mental and behavioral activities. The research areas that are committed to defining its functions every day range from neurophysiology to neuropsychology.

At the current state of research, it is believed that the brain acts both through structures and systems that are sufficiently well defined on the anatomical and functional level, and through an interneuronal network; a lattice involving the majority of neurons. This network acts on different levels of complexity, establishing contacts between the different levels of the entire cerebrospinal axis, up to single neurons.

The two cerebral hemispheres sometimes have equivalent, sometimes complementary functions: both preside over the motor, sensitive and sensory activities of the contralateral hemisome; the left hemisphere has a dominant role as far as language and conceptualization are concerned, just as the right hemisphere has it in verbal visuo-spatial functions and in the recognition of emotions. At the cortical level, zones (primary, secondary, accessory areas) have been identified which preside over the various somatic activities. The primary motor area was the first to be identified over time; corresponds to the ascending frontal or pre-central gyrus. In this the localizations of the motility of the foot, of the lower limb, of the trunk, of the upper limb, of the hand, of the eyes, of the face and those connected with the vocalization, the mastication and the swallowing follow one another: the dimensions of the associated with the control of each muscle district, are greater the finer the movement of the same district. The secondary and accessory motor areas are both located in the adjacent

premotor cortex. These areas manage coordinated movements, which are less basic than those of the primary area.
The cortical projections of the various forms of sensitivity, olfaction excluded, occur by fibers that have their origin at the diencephalic or brainstem level: in the optic thalamus (fibers for general sensitivity, minus the pain ones, and with the probable addition of the gustatory ones), in the medial geniculate body (acoustic fibers), in the lateral one (visual fibers), in the vestibular nuclei of the medulla oblongata (vestibular fibers). The general sensitivity, excluding the nociceptive one, has the primary projection area in the ascending parietal gyrus, or post-central, the secondary one on the upper lip of the Silvian fissure. Hearing projects into the superior temporal gyrus: both in the primary area, both in the secondary one the activities are topographically correlated with those of the different coils of the cochlea (tonotopic organization of the cortex). In the same convolution the vestibular sensitivity is projected, anterior to the acoustic areas. Vision projects onto the labia of the calcarine fissure and onto part of the adjacent surface of the occipital pole. Recent studies place the seat of taste in the lower zones of the two pre- and postcentral convolutions, superimposing on the tactile activities coming from the tongue. Lastly, olfactory sensations are projected into the cortex of the convolution of the olfactory trigone and into the cortex next to the amygdala via the neurites of the mitral cells of the olfactory bulb. Connections depart from the amygdala in the direction of the reticular substance, the thalamus, of the hypothalamus and to the frontoparietal cortex. The thalamus, exploiting its nuclei, intervenes in multiple functions: with the sensory connecting nuclei it sends most of the information coming from the body and from the external environment to the cortex; it intervenes in the conscious processing of painful stimuli and, through the limbic system, in emotional dynamics; in connection with the cerebellum, with some formations of the base and with the cerebral cortex, it participates in the control of the execution of the movements, it is hypothesized that it is responsible for the mechanism of their initiation. The functional role of the hypothalamus is extremely complex; it plays a prominent role in the control of the vegetative functions, which it performs both with the mechanisms of the nervous organs and through humoral mechanisms. Furthermore, a considerable part of hypothalamic neurons associates morphological and functional properties, common to all nerve cells (action potentials, synaptic mechanisms), with other functional characteristics, such as secretory activity and sensitivity to environmental stimuli of various kinds: thermal, osmotic, humoral

(thermo, glycose, steroid, osmo sensitive neurons). In endocrine activity, the hypothalamus participates with the magnocellular and parvicellular neurosecretory systems. The former processes oxytocin and vasopressin which flows into the neurohypophysis with the hypothalamic-pituitary fascicle; the second elaborates particular hormonal substances, the release factors and the inhibition factors, which control the secretion of corresponding hormones by the anterior pituitary gland, which they reach through the venules of the hypothalamic-pituitary portal system. Other interventions of the hypothalamus concern the control of lactation, thermoregulation, the intake of food through the hunger and thirst centers, sexual activities and emotional control.

The central nervous system (CNS) is made up of two classes of cells: glial cells and nerve cells called neurons.

Glial cells have structural functions, they support and separate groups of neurons. The neuron is the basic unit of the central nervous system.

3.2.1 The Neuron

The neuron is an excitable cell capable of receiving, processing and transmitting information to adjacent cells by means of impulses, known as an action potential or spike.

Structurally, the neuron has a cell body or soma (Fig 1.2), within which it is possible to identify the nucleus of the cell separated from the rest of the cell and other organelles responsible for the main cellular functions.

Both dendrites and axons are types of cytoplasmic extensions that branch out from the main body of the cell. Dendrites, which have the appearance of tree branches, are responsible for sending out signals in a radial manner after receiving them from afferent neurons. Instead of sending the signal in a straight line, the axon will send it out in a circular pattern so that it may reach more cells. A membrane on its outside is responsible for both its consistent diameter and its strong conductivity (neurolemma or sheath).

both internal and external factors (Schwann and the (myelin sheath). These membranes create a layer of insulation that shields the axon and protects it from damage. There are bottlenecks at various points along the neurolemma, which are places where the myelin sheath becomes damaged. A protrusion at the very tip of the axon is known as the terminal button. The terminal buttons on an axon make it possible for the axon to make contact with the dendrites or cell bodies of nearby neurons, which is necessary for the transmission of a nerve impulse via the neural circuit.

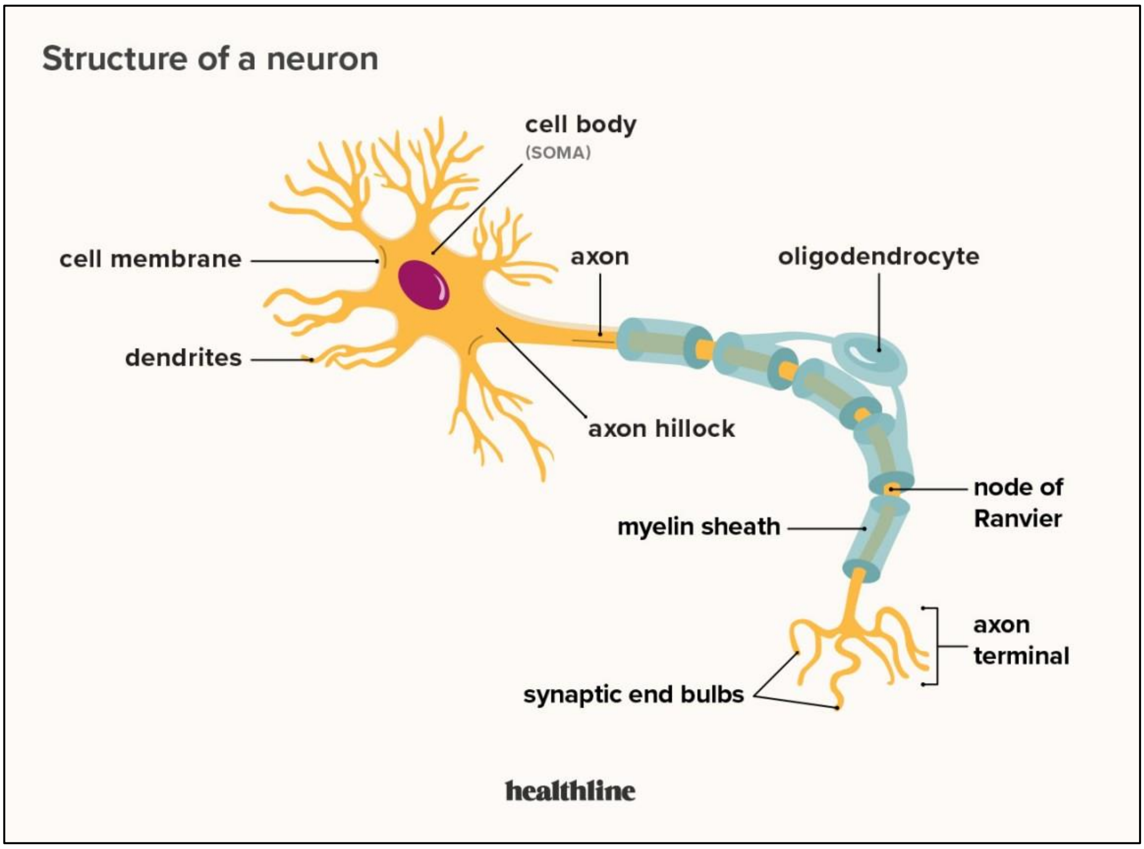

Figure 3.2: Neuron Structure.

3.2.2 Alzheimer’s Disease

Alzheimer's disease is a complex and progressive neurodegenerative disorder that primarily affects cognitive functions, memory, thinking, and behavior. It is the most common cause of dementia, accounting for approximately 60-70% of all dementia cases. The disease was first described by Alois Alzheimer, a German psychiatrist and neuropathologist, in 1906.

Here's an extensive explanation of Alzheimer's disease:

Symptoms and Stages:

Early Stage: In the early stages, individuals may experience subtle changes in memory and cognitive function. They might have trouble remembering recent events, names, and conversations. Concentration and problem-solving abilities can also be affected.

Middle Stage: As the disease progresses, memory loss worsens, and individuals may have difficulty recognizing family members and close friends. Language problems and behavioral changes become more noticeable. Activities of daily living (ADLs) such as dressing, eating, and bathing might become challenging.

Late Stage: In the advanced stages, individuals lose the ability to communicate and require assistance for even the most basic tasks. They may become immobile and vulnerable to infections. Eventually, Alzheimer's can lead to severe physical and mental impairment, often requiring round-the-clock care.

Causes and Risk Factors:

Age: Age is the primary risk factor. The likelihood of developing Alzheimer's increases significantly after the age of 65.

Genetics: A family history of Alzheimer's increases the risk, and specific genes such as APOE-e4 have been associated with higher susceptibility.

Amyloid Plaques and Tau Tangles: Alzheimer's is characterized by the accumulation of abnormal protein aggregates in the brain. Amyloid plaques, composed of beta-amyloid protein, and tau tangles, involving the tau protein, disrupt neuronal communication and lead to cell death.

Pathophysiology:

The exact cause of Alzheimer's is still not fully understood, but there is growing evidence that multiple factors contribute to its development. Genetic, environmental, and lifestyle factors all play a role.

Abnormal processing and accumulation of amyloid beta protein lead to the formation of plaques, which disrupt communication between neurons.

Tau protein undergoes abnormal modifications, leading to the formation of neurofibrillary tangles. These tangles disrupt the internal structure of neurons, impairing their function.

Diagnosis:

Alzheimer's diagnosis is primarily clinical, based on a comprehensive assessment of a person's cognitive function, memory, behavior, and daily activities.

Brain imaging techniques, such as MRI and PET scans, can reveal structural changes and the presence of amyloid plaques.

Neuropsychological tests and biomarker analysis (like cerebrospinal fluid examination) can aid in diagnosis and tracking disease progression.

Treatment and Management:

Medications: While there is no cure for Alzheimer's, medications such as cholinesterase inhibitors and memantine can help manage symptoms, providing temporary relief in some cases.

Non-Pharmacological Approaches: Cognitive stimulation, physical exercise, social engagement, and a healthy diet may slow down cognitive decline and improve quality of life.

Supportive Care: As the disease advances, individuals often require assistance with daily activities and may need to move into specialized care facilities.

Research and Future Directions:

Ongoing research is focused on understanding the underlying mechanisms of Alzheimer's and identifying potential drug targets.

Early detection through biomarkers and genetic testing could enable interventions before significant brain damage occurs.

Advances in precision medicine and personalized treatment approaches are being explored to develop more targeted therapies.

3.3 ACQUISITION OF BRAIN SIGNALS

3.3.1 Electroence Phalography

The EEG consists in measuring the difference in electrical potential between pairs of electrodes, one active and one reference insensitive to the measurement of interest (Figure 3.3).

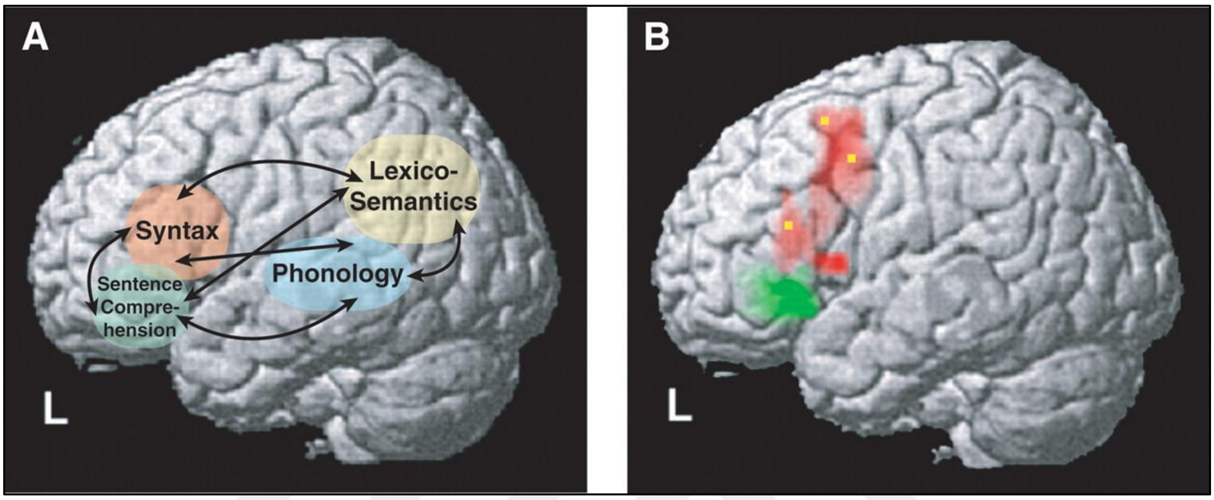

Figure 3.3: Acquisition of Brain Activity Between Two Sites.

Ideally, the reference electrode is sensitive to changes in signal in the same manner as other electrodes; this characteristic allows to subtract from the signal recorded by the electrodes, what does not properly represent the cerebral electrical activity. The reference electrode should also not acquire activity from external sources, such as cardiac activity; generally, these electrodes are placed in the earlobes, in the tip of the nose or in the mastoid bones.

Active electrodes may either be placed directly on the surface of the scalp or they can be incorporated into a scalp-adherent elastic cap, although this decision is made according to the duration of the clinical observation. The contact between the electrode and the scalp takes place by means of a conductive gel which is introduced at the level of the sensors after positioning the headset.

The number of electrodes placed in the headset is variable; Headphones with up to 256 electrodes are commercially available.

In order to guarantee the comparison between the results of different studies, the positioning of the electrodes must necessarily follow a standard. For this reason, the surface electrodes are placed on the scalp following the positioning indications of the International 10-20 System. This system provides for the arrangement of electrodes with even numbers on the right hemisphere of the skull and electrodes with odd numbers on the left side. Each electrode bears the indication of the initial letter of the skull bone over which it is placed.

In the event that the number of electrodes is greater than 32, it is common practice to use the average reference, for example by subtracting the average value, estimated among all the electrodes, from the signal recorded by each electrode in each single instant of time.

In case the single reference electrode was used during the recording, it is possible to re-reference it later during the signal pre-processing phase. A further type of referencing is obtained by using bipolar recordings, for example in the case in which pairs of electrodes are referenced with respect to the rest of the pairs (e.g. symmetrical pairs of electrodes between the right and left hemisphere).

The amplitude of the amplitude of the measured signal is of the order of 50 μV; an amplification and digitization of the signal is necessary in order to be pre-processed and used for subsequent investigations.

3.3.2 Magnetoence Phalography

The amplitude of the magnetic field produced by brain activity is of the order of the pT when it is acquired; this activity is recorded through superconducting rings called "SQUIDS" (Superconducting Interface Devices) which are crossed by the magnetic flux. The magnetic field has a direction, defined by the field lines. The ring only measures the strength of the magnetic field directed perpendicular to itself. For the purpose of measurement, different configurations of rings are used. A single ring is called a "magnetometer". If the difference in signal between two or more neighboring rings is measured, we speak of a first-order "gradiometer", second-order, and gradually increasing as a function of the number of rings. The characteristic of the gladiometers is that they are not very sensitive to sources located at great distances. This has the direct advantage that noise sources at great distances, such as cardiac activity or activity generated by nearby devices, are suppressed.

As previously mentioned, a characteristic of magnetoencephalography is its insensitivity to radial current sources, perpendicular to the scalp. What is measured are tangential sources, parallel to the scalp.

To fully grasp this concept, it is necessary to imagine the head as the representation of a sphere; the recording ring is placed tangentially to its surface. The activity of a small area of the cortex assumes the behavior of a dipole. A "tangential" dipole generates a magnetic field parallel to the scalp surface while a "radial" dipole can point towards or away from the scalp (Figure 3.4).

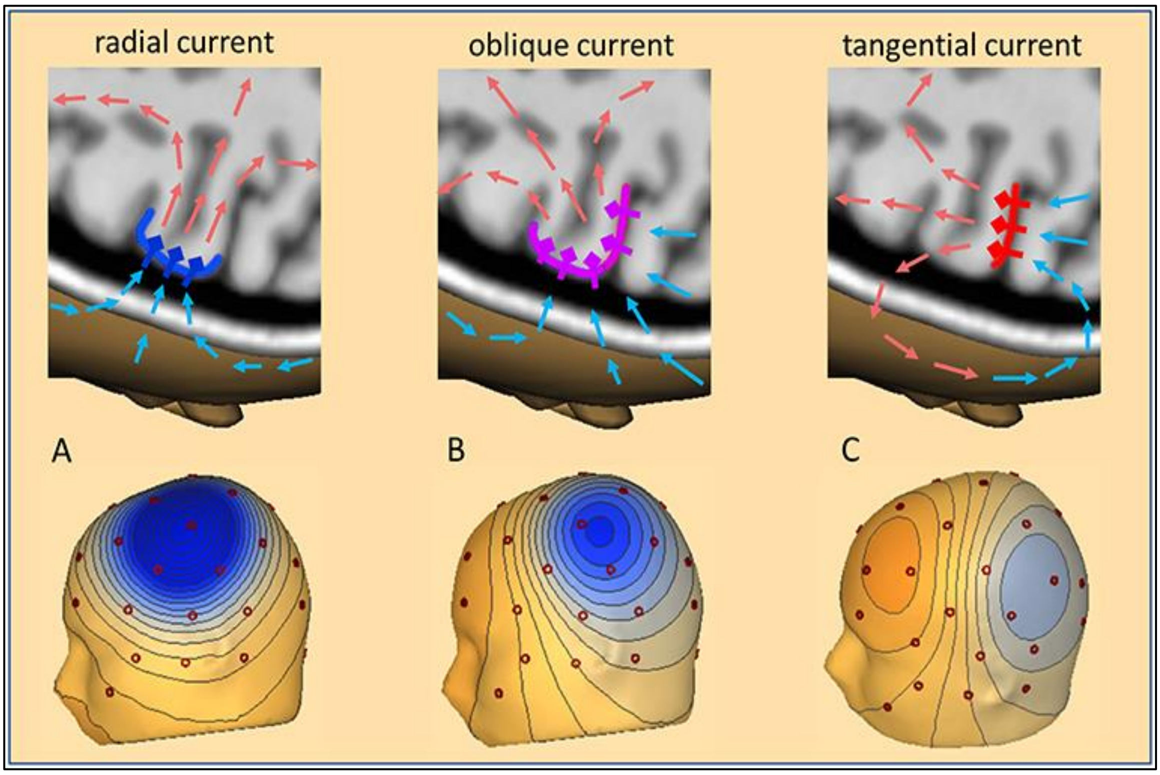

Figure 3.4: Tangential (Top) and Radial (Bottom) Dipole.

A radial dipole pointing towards the scalp will produce a magnetic field parallel to the magnetometer and therefore its activity will not be recorded; the volume currents on the other side are symmetrical with respect to the axis indicating the direction of the dipole. This means that the magnetic field that passes through the ring on one side is canceled by the current on the opposite side. This happens for any recording site in case the dipole is radial. A particular case of radial dipole is a dipole positioned in the center of the sphere: it necessarily points outwards from the center and is invisible during the MEG.

3.4 BRAIN WAVES

Neural electrical activity varies among individuals, regardless of their health status. However, variations are also recorded in the same individual on the basis of the activity carried out; for example, the trace appears different if recorded in waking or sleeping conditions.

The oscillations of the electric potential are called brain waves. Each brain frequency is associated with different cognitive functions.

Based on the frequency of the observed signal (Figure 3.5).

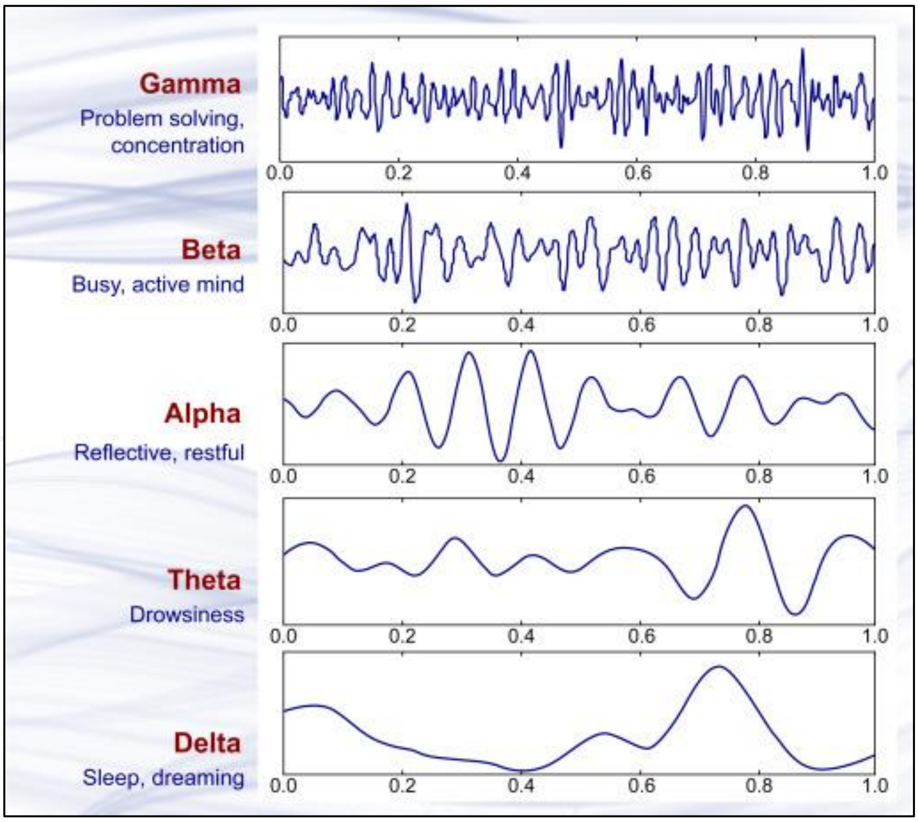

Figure 3.5: Types of Brain Waves.

Delta waves: (0.5 and 4 Hz) in adulthood they occur during deep sleep and in some encephalic pathologies; are the dominant waves in newborns.

Theta waves: (4 and 8 Hz) represent the dominant rhythm during the neonatal period.

In the adult they are present in the case of cerebral pathologies, in states of hypnosis and emotional tension.

Alpha waves:(between 8 and 13 Hz) are the waves present in the brain activity of subjects in the state of wakefulness in conditions of cerebral rest with eyes closed.
Beta Waves:(13 and 30 Hz) is the fastest rhythm and is divided into slow beta (13 Hz- 20 Hz) and fast beta (20 Hz- 30 Hz). They are dominant during any brain activity in a subject with eyes open.
Gamma Waves:(30–90 Hz) several studies associated the gamma band with visual attention, perception, memory and pathologies such as epilepsy, atism, ADHD (attention deficit disorder) and schizophrenia.
Studies conducted in the last decade have hypothesized that the oscillations recorded by electroencephalography considering frequencies >20 Hz, reflect artifacts of a muscle type.

3.5 DEEP LEARNING-BASED APPROACHES TO RECOMMENDATION

As we have seen, recommender systems are used to generate educated predictions about the likelihood of delight experienced by consumers for material that they have not yet viewed. These informed estimates are based on historical data. The three basic responsibilities that fall under the category of recommendations are rating prediction, classification prediction (top-n suggestions), and categorization. The goal of the rating prediction task is to fill in the gaps in the item-user rating matrix with the appropriate values. Topn creates a ranked list of n items that is unique to the user and is based on their recommendations. The next thing that has to be done is some kind of classification, which will include placing prospective suggestions in the appropriate categories.
We have gone through the three primary classification schemes that may be used for recommendation models. There are three distinct classifications that may be used to recommender systems: collaborative filtering, content-based, and hybrid. The purpose of collaborative filtering is to provide recommendations to users and products based on their previous interactions with one another. Ratings from users are an example of an explicit kind of input, while popularity is an illustration of an implicit form of feedback (e.g. browsing histories). It is common practice, when making a proposal based on the content of an article, to evaluate various parts of the article and make use of supplementary data offered by users before coming to a final decision on what, if anything, should be recommended. This is done before coming to a conclusion on whether or not anything should be recommended. The most beneficial aspects of each of these approaches, in addition to other

aspects, are combined in hybrid approaches. However, it is important to keep in mind that, from a more holistic perspective, a large amount of extra data, which may include texts, images, and videos, may be taken into account in order to further improve the prediction capacity of the model.

In this section, we are going to have a look at a variety of different architectures for DL learning, talk about the problems that each one solves, and go through the techniques that each utilize.

To get things started, I'll go through the notation that will be used for the whole of this work. In the sake of keeping things as simple as possible, let's suppose that R is the evaluation matrix and that M users rated N items on a scale from 1 to 5. There is a vector r(u) for every user u, and it is made up of the numbers ru1 through ruN. Additionally, there is a vector r(i) for every item I, and it is made up of the numbers r1M through rMi. In this part of the discussion, we are going to take a cursory look at the notations and their associated explanations that are going to be utilized in the next parts of the conversation.

a. R: ratings matrix
b. M: number of users
c. rui: rating of item i given by user u
d. r(i): partially observed vector for item i
e. U: latent factor of the user
f. $\mathcal{O}$,$\mathcal{O}$-: Sets of observed or unobserved ratings
g. W*: Neural network weight matrix
h. R_: Matrix of predicted ratings
i. N: Number of items
j. rꜝ'': Predicted rating of item i, given by user u
k. r(u): Partially observed vector for user u
l. v:Vector of latent factors
m. K:The maximum rating value (explicit)
n. b*: Bias terms for neural networks

3.5.1 Deep Learning

Companies have typically relied on classical machine learning models for a variety of purposes, including credit scoring, churn prediction, consumer targeting, and others, due to the fact that these models allow for the effective management of structured data. The phase known as "feature engineering" is an essential component of the process of developing these models since it is at this stage that the essential information is derived from the structured data and applied to the model as input.

Within the realm of machine learning known as deep learning, artificial neural networks are often used. Within the framework of a deep learning model's layer structure, lower-level concepts are responsible for specifying higher-level ideas.

This article illustrates the possibilities of deep architectures in demanding AI problems and provides a strategy that simplifies the process of training deep models. Deep learning techniques are now being used to find solutions to a wide variety of problems in the fields of computer vision, natural language processing (for voice recognition and text mining), and data mining.

a. Neural Network

Deep Learning's fundamental building component is called a perceptron, and it functions as a substitute for the individual neurons that make up a neural network.

In order to train a network utilizing a finite collection of m inputs (such as m words or m pixels), we must first multiply each input by a weight (1,...,m), combine the weighted combination of inputs, add a bias, and then run them through a function of non-linear activation. This process is referred to as "weighted combination learning".

This produces the output*y*to.

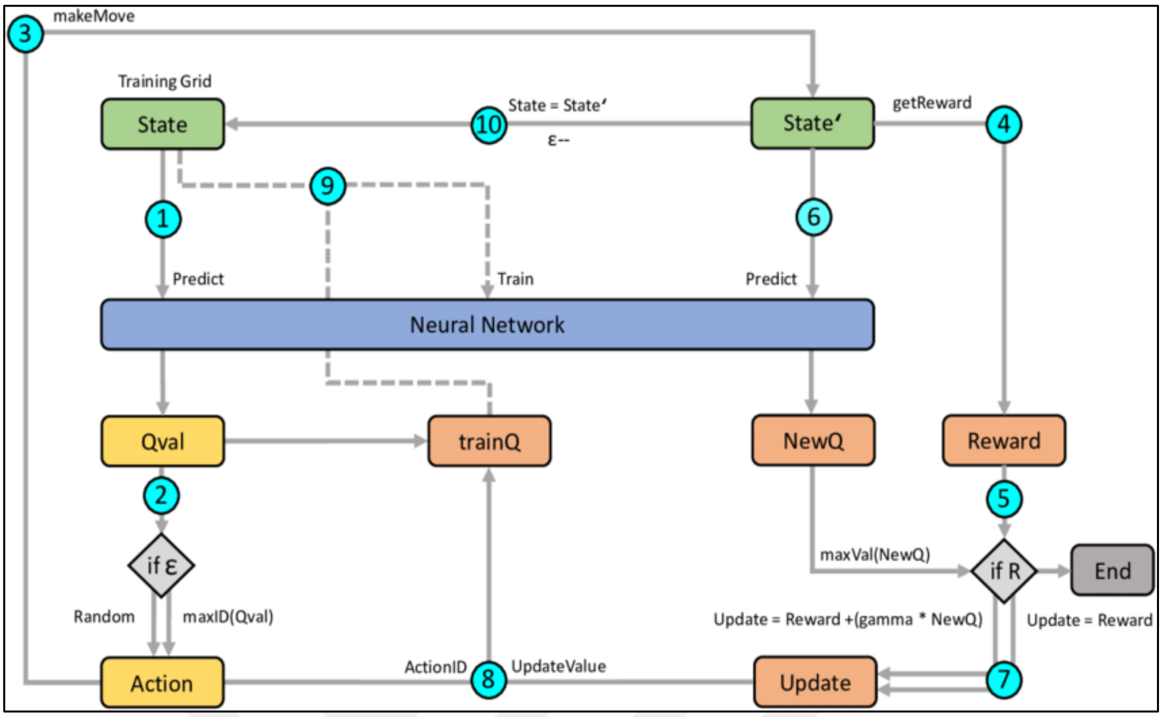

Figure 3.6: Learning Mechanism of a Neural Network.

i. You have the ability to add one additional axis to the input space if you use the theta bias. As a result, the activation function will still generate an output even if there is a vector of inputs that just contains zeros.

ii. Activation functions are what are employed to provide a network a non-linear pattern of behavior to exhibit. A linear activation function will always provide a linear option as the outcome, regardless of the distribution of the inputs. Because nonlinearity makes it easier to get a good approximation, even arbitrarily complicated functions can be described more accurately.

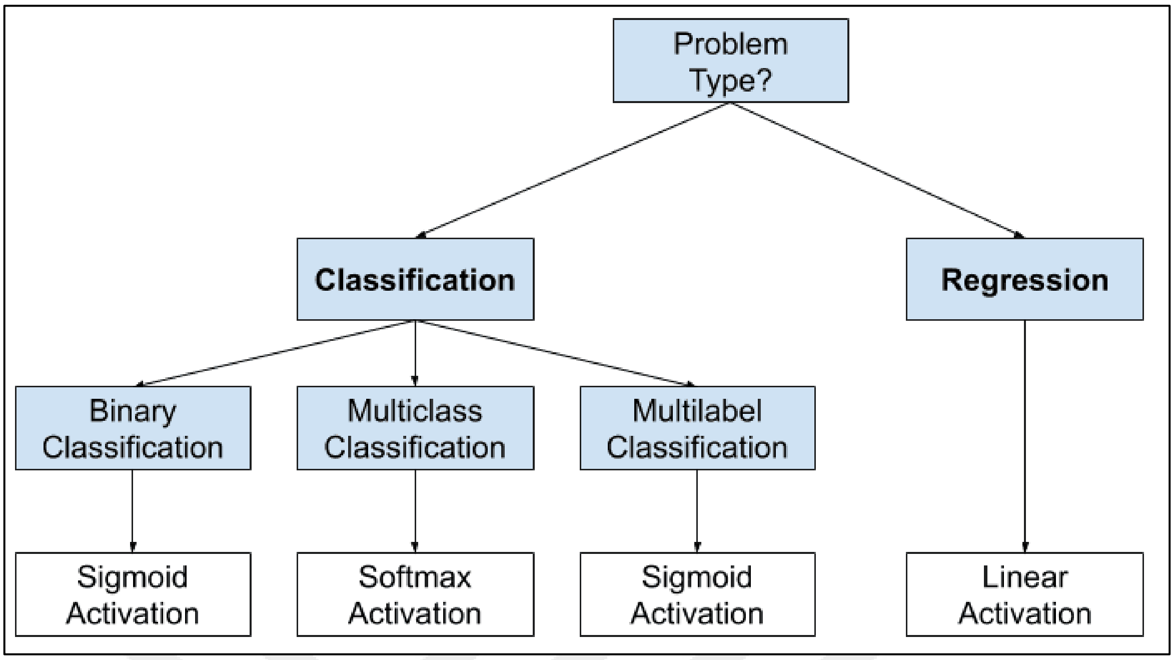

Figure 3.7: Main Activation Functions.

To simulate increasingly complicated functions, a deep neural network stacks numerous hidden layers on top of one another.

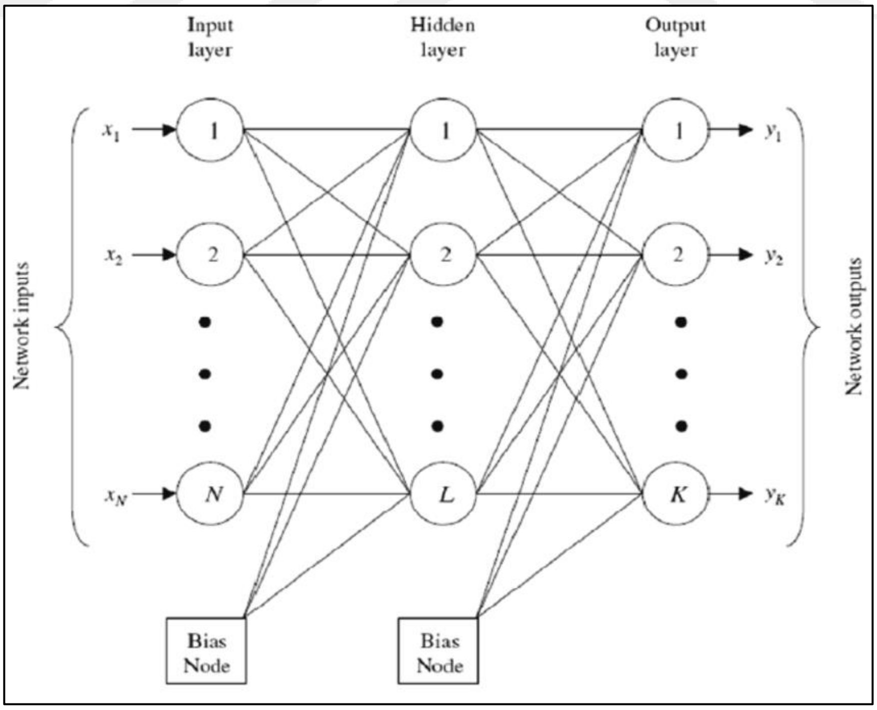

Figure 3.8: Diagram of a Neural Network.

3.5.2 Deep Learning Methods and Models for Recommendation

The great majority of their applications are found in different kinds of recommendation systems and deep learning models. The application of deep learning strategies to the problem of recommender systems is becoming an increasingly prominent and relevant trend. Deep learning gives you the ability to look at data from a variety of different sources, which makes it possible to identify previously unknown characteristics. Researchers have started implementing deep learning algorithms into recommender systems as big data technologies and supercomputers become more commonly accessible. The reason for this is that researchers have made significant strides in recent years regarding their capacity to process enormous volumes of data.

In particular, the use of deep learning methodologies has led to the identification of feasible solutions to some of the most significant challenges that are present in the field of recommender systems. These challenges include scalability and a lack of data. Two other uses of deep learning that may be found in the field of recommender systems are dimensionality reduction and the extraction of relevant attribute information.

Deep learning is used by recommendation systems in order to provide an accurate representation of the user-item choice matrix, content/side information, or both. Both of these tasks can be accomplished with the help of deep learning when applied in the appropriate contexts. In this section, we will explore the background of DL architectures in recommendation systems as well as the purpose they provide in order to have a better understanding of their application and implementation. In this section, many reference architectures, including RBMs, DBNs, autoencoders, RNNs, and CNNs, will be discussed in great length. It has been established that there is a vast diversity of cutting-edge models.

a. Multilayer Perceptron based Recommended System

The Multilayer Perceptron is an example of such an effective and condensed model. As a consequence of this, it is used in a wide range of areas, the most prominent of which is manufacturing. There is evidence to suggest that these networks are capable of approximating any measurable function to an accuracy of the user's choosing. It serves as the basis for a great deal of complicated modeling.

b. Neural collaborative filtering

As a general rule, recommendation is understood to be a two-way interaction between the preferences of a user and the attributes of a product. Matrix factorization, for example, may decrease the dimensionality of a rating matrix by first dividing it into two latent spaces, one for users and one for objects. This allows the matrix's overall size to be lowered.

c. Content-based recommender

The algorithm will build lists of content recommendations for the user based on the similarities found between their user profile and the attributes of the item.
As a consequence of this, it makes perfect sense to build a dual network that can accurately depict the mutually beneficial nature of interactions between humans and inanimate objects. Neural collaborative filtering is an example of one of these kinds of systems that attempts to capture the non-linear relationship that exists between people and things (NCF). The architecture of the NFC system is shown in the following figure 3.9.

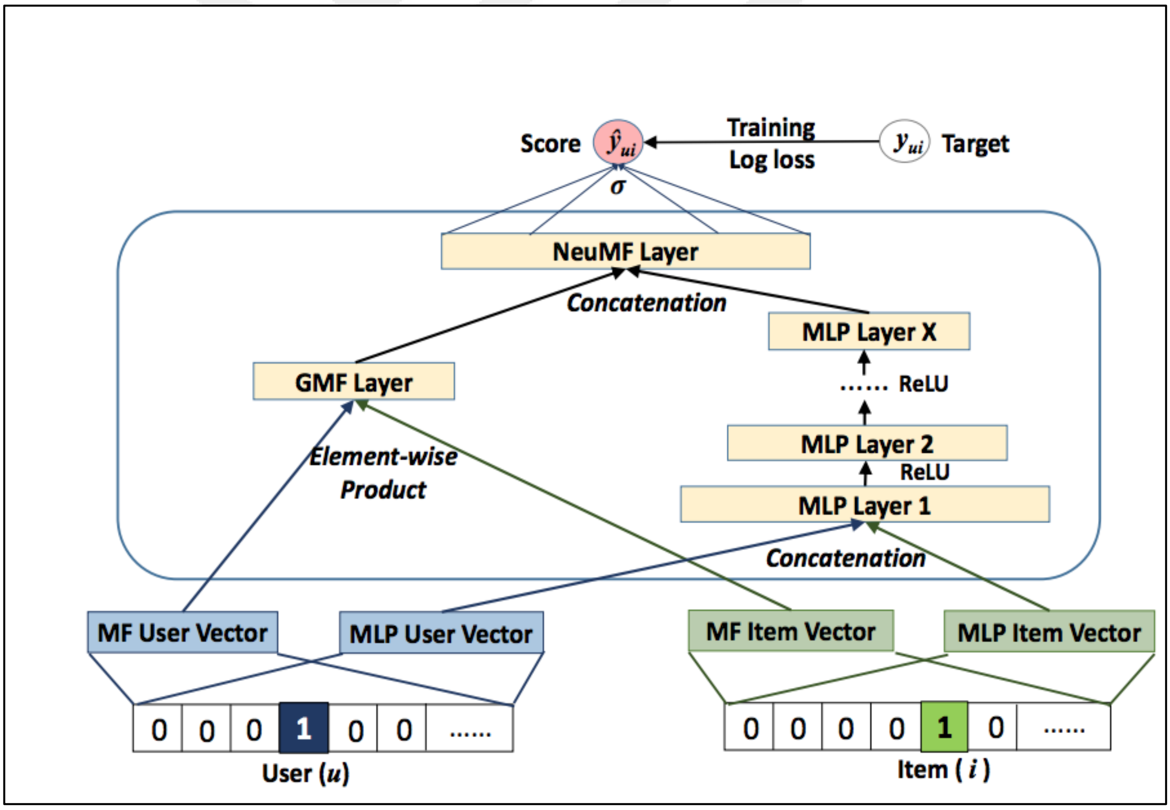

Figure 3.9: Neural Collaborative Filtering.

Assume that suuser and siitem are unique identifiers for the user and the item, or that they relate to supplemental data (such as user profiles and item characteristics). The following is the formula for the rule of prediction used by NCF:

$$\hat{r}_{ui} = f\left(U^T \cdot s_u^{user}, V^T \cdot s_i^{item} \mid U, V, \theta\right) \tag{3.1}$$

Where f(.) is the function of the multilayer perceptron and is the parameter for the network. For the purpose of making predictions about explicit evaluation, the loss function that is used is the weighted squared error.

$$\mathcal{L} = \sum_{(u,i)\in\mathcal{O}\cup\mathcal{O}^-} w_{ui}(r_{ui} - \hat{r}_{ui})^2 \tag{3.2}$$

Which aspect of wui is the training instance's significance going forward? (u,i). The authors suggested a probabilistic approach (such as the logistic function or the Probit) to restrict the rui output to the interval [0,1] and revised the loss to a form of cross-entropy. If the rating is a binary one (where 1 represents a like and 0 represents a dislike), then the loss should be reformulated as cross-entropy.

$$\mathcal{L} = -\sum_{(u,i)\in\mathcal{O}\cup\mathcal{O}^-} r_{ui}\log \hat{r}_{ui} + (1 - r_{ui})\log(1 - \hat{r}_{ui}) \tag{3.3}$$

Because there are such a large number of unobserved events, NCF uses a technique called negative sampling to significantly reduce the amount of simplified data. This has the effect of significantly boosting the efficiency of the learning process. It is possible to grasp the concept of classical matrix factorization as a particular illustration of NCF. In order to make more effective use of the linearity of matrix factorization and the nonlinearity of MLP in order to improve the overall quality of the proposals, it is practicable to combine matrix factorization with NCF in order to build a more general model.

In this article, we describe a neural social collaborative ranking recommender system that extends the NCF model to provide recommendations to users across other domains, such as the ones found on social networks. Specifically, the system ranks and recommends users' favorite content based on how well it collaborates with other users. As shown in Figure 3.10, one example of this category is a CCCFNet, which stands for a cross-domain content-boosted collaborative filtering neural network.

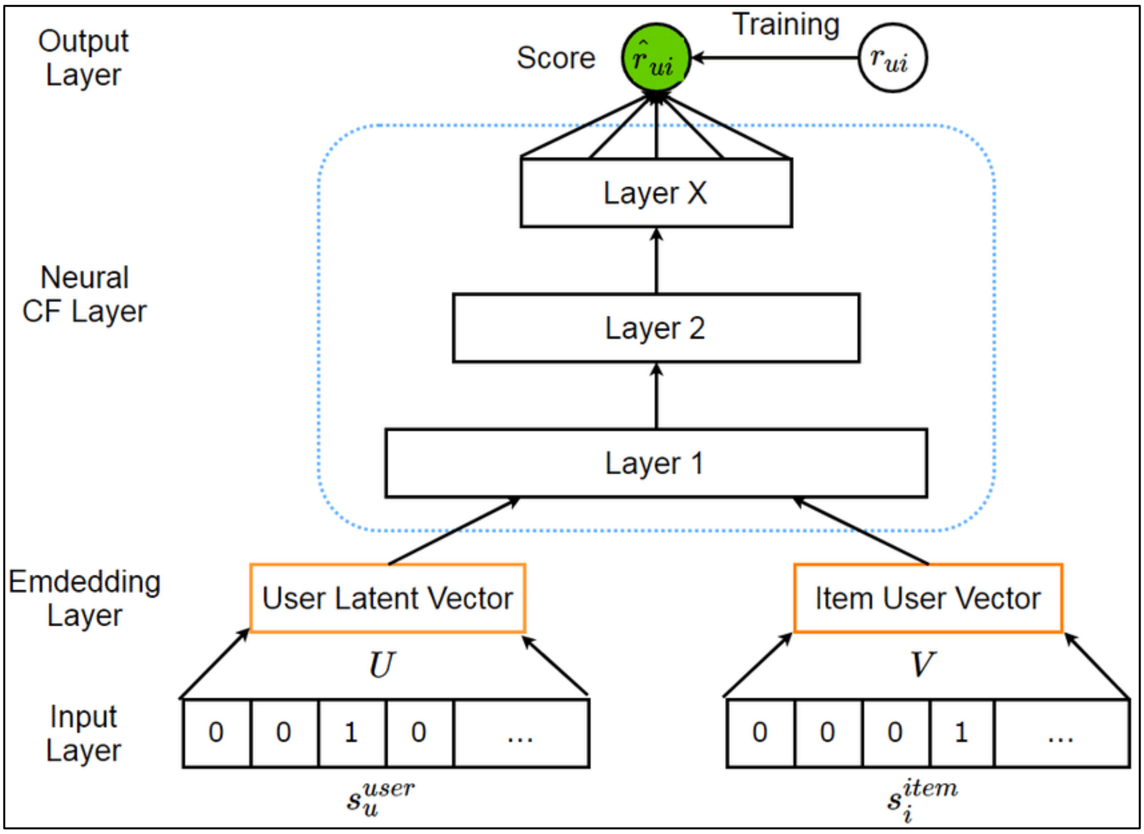

Figure 3.10: Cccfnet.

Similarly, to how the basic component of CCCFNet is a double network (respectively for users and items). The interactions that take place between the user and the product are modeled using a dot product at the very top layer of the structure. After that, the writers went over each network to offer specifics on the material (belonging to the dual network).

a. multi-view neural framework is defined from the base model to make cross-domain recommendations.

d. Large and Deep Learning

This model is represented in the following figure.

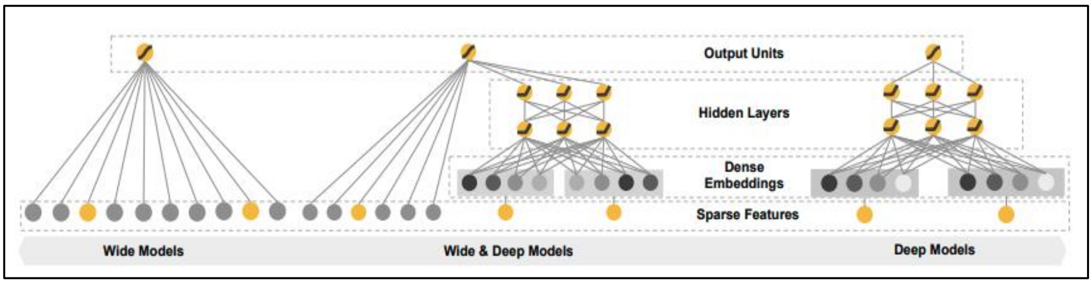

Figure 3.11: Wide & Deep Learning Combination.

Although the model was first presented for the purpose of making app recommendations on Google Play, it is adaptable enough to be used for regression as well as classification problems. Deep learning is accomplished via the use of a multilayer perceptron, while wide learning is accomplished through the use of a single layer of many perceptrons (or a generalized linear model). Combining the two approaches to learning has the potential to provide the recommender system with the capacity to take into consideration both the short-term memory and the long-term retention of information. You will be able to recall a lot of knowledge with the aid of the wide learning component, which is similar to learning how to grasp specific aspects from historical documents. In the meanwhile, the deep layer is responsible for recording the generalization, which results in representations that are both more abstract and complete.

This technique has the ability to improve the accuracy as well as the diversity of the suggestions.

e. Deep Factorization Machine

A DEEPFM is represented in the following figure.

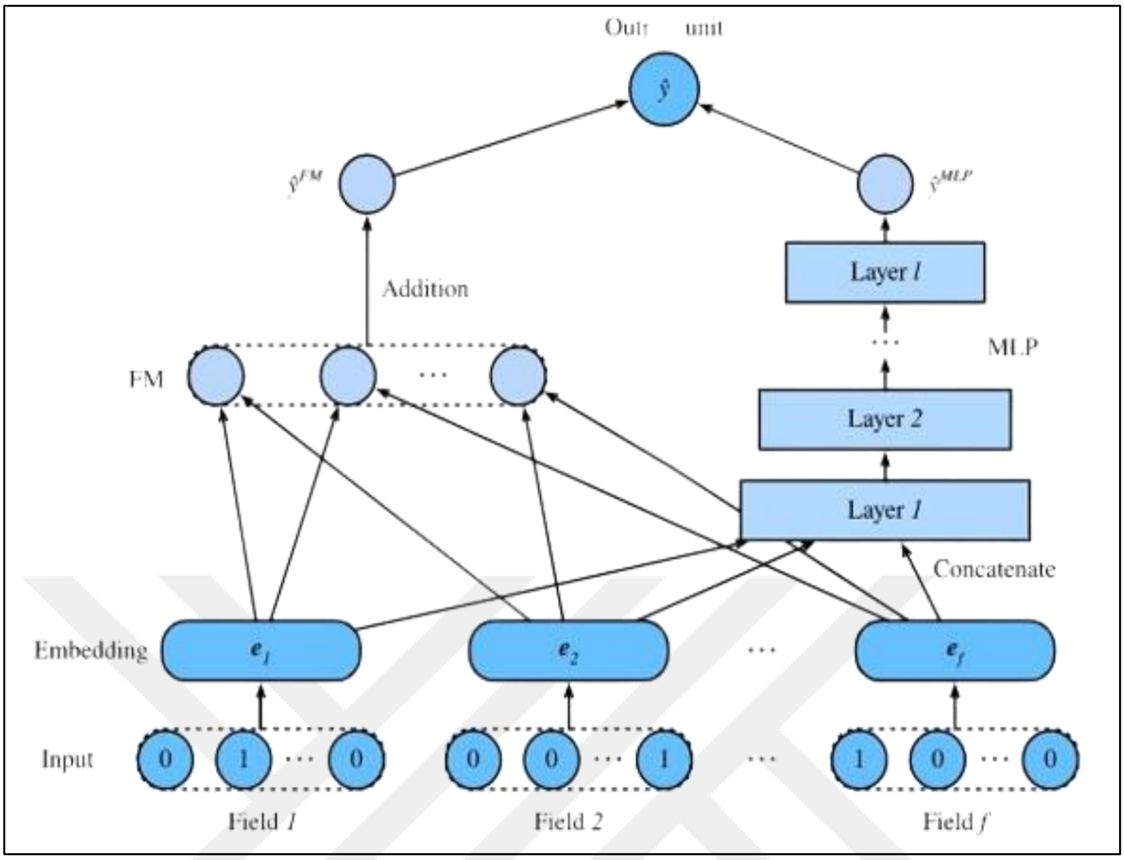

Figure 3.12: Deepfm.

DeepFM is a model that covers a lot of ground since it combines two different types of neural networks into one: the factorization machine and the multilayer perceptron. The accuracy of the prediction will ultimately be enhanced as a consequence of this. The factorization machine is used to provide an explanation for low-order interactions, whilst a deep neural network is used to provide a simulation of high-order interactions. In order to do its computations, the factorization machine makes use of both addition and the inner product.

MLP makes use of nonlinear activations and sophisticated structures in order to describe higher-order interactions. The combination of these two different kinds of models has been shown to be successful thanks to the existence of a large and well-connected network. DeepFM, on the other hand, doesn't need any kind of specialized feature engineering as the wide and deep model requires. A matrix of u, I pairs serves as the input for the DeepFM algorithm, where m denotes the total number of fields (the identity and characteristics of user and item). For ease of writing, the outcomes of FM and MLP analyses are often expressed as yFM(x) and yMLP(x). The prediction score is comprised of many components, including the following ones:

$$\hat{r}_{ui} = \sigma(y_{FM}(x) + y_{MLP}(x)) \tag{3.4}$$

Here, sigmoid activation function (.) stands in for everything else.

F. Attentive Collaborative Filtering

The visual attention that humans possess provides a source of motivation for the act of focusing. For example, the only way for humans to interpret visual inputs in their whole is to concentrate their attention on certain parts of them. It's possible that the attention mechanism will filter out any noise and any information that isn't essential from the inputs. The attention-based method has shown to be beneficial in a variety of applications, including speech recognition and machine translation, amongst others.

In recent studies, recommendation models that make use of deep learning techniques (such MLP, CNN, and RNN, for example) have shown promising results. [Citation needed] a model of latent components with a two-tiered attention filtering process that is group-based and uses collaborative effort. The attention model, which is an MLP, is constructed up of several elements and components.

The aspects of a user's experience that are given the most attention reveal the most important aspects of their personality. The purpose of this analysis at the component level is to glean from the additional multimedia data the most relevant information pertaining to each individual user.

3.5.3 Autoencoder-Based Recommender Systems

The data that is received from the encoder subnet is compressed using a rudimentary autoencoder before being sent on to the decoder subnet. In this scenario, the information is uncompressed and restored to its original form by the decoder network component. The output data from an autoencoder should be able to be patched back together to recreate the original data. This is the purpose of the autoencoder. These models are used in recommender systems to first learn a non-linear representation of the matrix and then rebuild it. This is done so that the user-item matrix may be filled in with the appropriate information.

Other uses for autoencoders include the reduction of dimensionality in data and the extraction of latent vector feature sets. In order to do this, the output values of the encoder are utilized.

It is possible to train (sparse) autoencoders with the help of sparse coding, and these autoencoders may subsequently be used to extract even more helpful features. When compared to incomplete sparse autoencoders (DAE), which place limits on the representation, denoising autoencoders (DAE) make it possible to alter the reconstruction criteria, which in turn makes it possible to extract a representation that is at least acceptable. In actual operations, DAEs are given data that is flawed in some manner, and they are instructed to recreate the data from scratch. The primary purpose of this sort of model is to rectify inaccurate input.

The SDAE is constructed by stacking a large number of autoencoders. Autoencoders allow for the uncovering of a broad range of previously hidden properties, which may be done in a number of ways. Denoising autoencoders, also known as DAEs, have been used into recommender systems in order to estimate missing values based on corrupted input. SDAEs contribute to the discovery of a more condensed representation of the input matrix when they are used in combination with recommender systems.

They make the process of acquiring information from a wide variety of sources simpler and may be put to use to integrate and give additional data.

Research carried out in this field employing autoencoders reveals that the recommendations that are generated as a consequence are more accurate than those that are generated by RBMs. This is due to the fact that the goal of autoencoders is to reduce the root-mean-squared error in their predictions, but the objective of RBMs is to increase the loglikelihood. The training process for autoencoders uses gradient-based backpropagation, while RBMs rely on contrastive divergence. As a result, autoencoders may be taught a great deal more rapidly than RBMs. The predictions that are generated by stack-aware autoencoders are more accurate than those generated by non-stack autoencoders due to the fact that stack-aware autoencoders enable in-depth learning of hidden properties.

a. Autorec

AutoRec will accept as input either the partial vectors r(u) that belong to the user or the partial vectors r that belong to the element in order to reconstruct the input layer (i). It seems as if there are two separate forms, one for user-based input and another for item-based input, with the latter being designated as "I-AutoRec" (U-AutoRec). Only IAutoRec is shown here, however U-AutoRec may be inferred from it in an uncomplicated way thanks to its presence. The I-AutoRec structure may be seen broken down into its component parts in the accompanying figure.

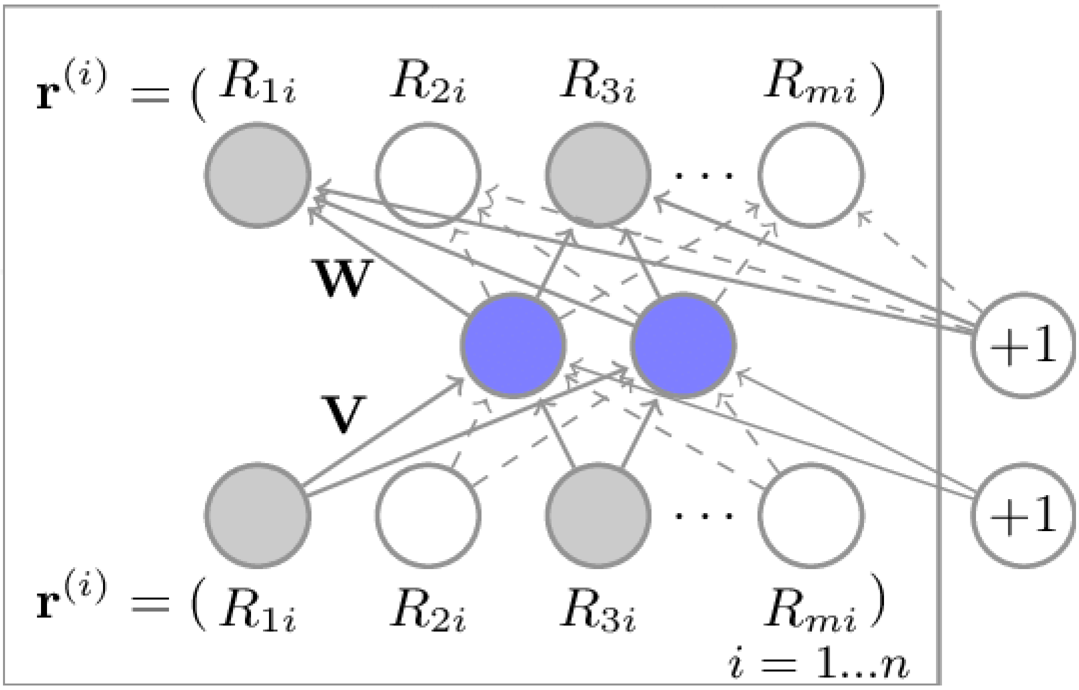

Figure 3.13: Autorec.

Input r(i) may be reconstructed using the formula h(r(i);) = f(W. g(V. r(i) +) + b, where f(.) and g(.) are activation functions and = W, V,, b. I-goal The following describes the purpose of AutoRec:

$$\underset{\theta}{\arg} min \sum_{i=1}^{N} \|\mathbf{r}^{(i)} - h(\mathbf{r}^{(i)}; \theta)\|_{O}^{2} + \lambda \cdot \text{ Regularization} \qquad (3.5)$$

This indicates that only the actual ratings are relevant. The objective function can be optimized more effectively thanks to resilient propagation (converges faster and produces comparable results).

3.5.4 Restricted Boltzmann Machines for Recommendation

The Renormalizable Boltzmann Machine, often known as an RBM, is one example of the several types of Boltzmann Machines that are in use today. They are made up of the softmax layer, which is visible, as well as a second layer, which is not. Within an RBM, the layers do not communicate with one another in any way. In the realm of proposals, they are used to uncover heretofore undisclosed aspects related with client preferences and product assessments.

In addition, RBMs are used to jointly model the relationship between a user's voted-for items and the association that those things have with other users. This is done by combining the information from both sets of users. The accuracy of a recommender system may be improved by doing this, making it even more precise. RBMs are used by recommender systems that cater to groups in order to simulate the preferences of the group as a whole. In order to do this, it is required to simultaneously replicate both the dynamics of the group as well as the features of the individuals.

Because of the connections between the hidden layer and the softmax layer as well as the connections between the I softmax layers, it is possible to extract not only the link between an evaluated component and its rating but also the correlations between the components that were assessed. This is made possible thanks to the connections between the hidden layer and the softmax layer.

Boltzmann machines, which are used in recommender systems, are responsible for displaying the pairwise correlation that exists between users and objects. It is recommended to make use of Boltzmann machines for modeling user-item connections as well as when merging content data. In particular, information on the contents is connected to features of the equipment.

The ability of RBMs to provide a low-rank representation of user preferences is one of its most significant applications. On the other hand, Boltzmann machines are used to generate "neighborhoods" inside observable layers. These neighborhoods incorporate correlations between pairs of consumers or things. As RBM examines the connections between individuals and objects, we may end up developing a model that is a crossbreed, in which two visible layers are connected to one that is hidden from view (one for items and one for users).

In conclusion, RBMs, similar to Boltzmann Machines, may make use of supplemental information drawn from a broad variety of sources. This information may be included into the model.

3.5.5 Recommendation Approaches Based on Deep Belief Networks

In the realm of recommender systems, DBNs, also known as Deep Belief Networks, have been used to unearth information in audio recordings that had been buried for some time in order to more accurately recommend music based on the content of those songs.

In recommender systems and other applications that depend on textual data, DBNs are also employed. DBNs are also used as classifiers in content-based recommendation systems that operate with text.

In addition to that, DBN may be used to provide a semantic representation of words. The ability of DBNs to extract high-level features from low-level characteristics depending on the selections made by the user is an additional benefit offered by these networks. These studies show that DBNs really excel when it comes to feature extraction, particularly from material that is written or spoken.

3.5.6 Recurrent Neural Networks for Recommendation

The processing of data in sequences is where recurrent neural networks, also known as RNNs, shine. The most recent browsing behavior of a user is a factor that is considered while making purchase selections at an online retailer. Most recommender systems end up disregarding the actual order in which the user does activities since user preferences are created at the beginning of a session. This is because most users create their preferences right away. The accuracy of recommender systems may be improved with the use of a technology known as recurrent neural networks (RNNs), which take into consideration both the user's historical behavior as well as their current behavior when they are surfing the web. When producing predictions, the output of a feed-forward neural network is mixed with that of a recurrent neural network (RNN) in order to take into consideration user-item correlations. Recurrent neural networks are used to capture temporal and contextual features of user activities. These representations are then combined with latency variables that relate to user preferences in order to improve the accuracy of predictions. This process helps to improve the accuracy of predictions.

use RNNs to include customers' ever-evolving tastes into the recommendation process by seeing it as a set of prediction problems to be solved by the network. Last but not least, recurrent neural networks (RNNs) are a great tool for modeling the preferences of users and taking into account the implicit actions they do during a session.

3.5.7 Use of Convolutional Networks in the Recommendation Process

Convolutional neural networks, as its name indicates, use a convolutional layer in at least one of their component layers to accomplish tasks such as item classification and image identification. Not only are convolutional neural networks helpful for image identification, but they may also be used to make recommender systems more effective.

They have been used in circumstances when direct user input is not available in order to extract latent qualities from audio data. This has been done with the goal of improving accuracy. Convolutional neural networks are put to use in text mining in order to uncover hidden properties. The use of convolutional neural networks has made it possible to record visual characteristics of users, which has resulted in the development of user profiles and, as a consequence, the production of suggestions. CNNs are used to extract latent features from pictures for the aim of constructing a mapping between quality and user preferences in the same latent space. This mapping is done in the same latent space. In addition, the semantic meaning of textual information that is gained by convolutional neural networks is used by recommendation systems, especially context-aware recommendation systems, in order to present options that are more correct. This is particularly true for recommendation systems that take the surrounding environment into consideration.

As a consequence of this, a number of recommendation systems have started making use of convolutional neural networks in order to accomplish the objective of extracting latent variables and features from data, in particular from pictures and text. Last but not least, a fresh line of inquiry is investigating how CNN may be used to investigate topics such as viewer preferences and ratings of products and services.

4. PROPOSED METHOD

4.1 WORK OUTLINE

This research focuses on raw EEG signals and extracted brainwave frequency bands in order to evaluate the effectiveness of deep learning architectures for both age categorization and age regression analysis. The purpose of this evaluation is to determine whether or not these architectures can accurately predict an individual's age. The purpose of this study is to establish whether or not such architectures are successful in achieving their goals. This article examines a number of distinct kinds of deep learning models, including long-term short-term memory (LSTM), gated recurrent units (GRU), bidirectional long-term memory (BLSTM), and bidirectional gated recurrent units (BGRU), for the purpose of determining whether or not they are practical and effective. Even though each model was built and tested, the GRU-based models were not included in the pertinent sections because their findings were so similar to those of the LSTM and BLSTM models. This decision was made despite the fact that all models were constructed and evaluated. Despite the fact that all of the models had already been built, this was still accomplished.

A recent development that has sparked the attention of scientists is the possibility of applying deep learning models to data obtained from a wide variety of techniques for recording the activity of the brain. Convolutional neural networks (CNNs) and T1-weighted magnetic resonance imaging (MRI) structural pictures have been used in a number of studies that have investigated the possibility of estimating the age of healthy individuals. One of these studies is Franke et al. [5,] which is an example of one of these studies. This was carried out with the purpose of establishing whether or not the people being tested suffered from any illnesses. The mean absolute error (MAE) was found to be 4.6 years when Qin et al. [6] compared the age that was actually present to the age that was projected by the fMRI data. Using MRI scans as their primary source of information, Lam et al. [7] suggested using a two-layer recurrent neural network model that was built on two-dimensional slices as a method to classify the age of the brain. Their model makes use of a 2D convolutional neural network (CNN) to encode MRI scan features and a recurrent neural network (RNN) to understand the relationship between these features. They were able to achieve a mean absolute error (MAE) of 2.8 years with this model [7].

In a different set of experiments utilizing CNNs, Truong et al. [16] used a dataset consisting of more than a thousand children to compare the efficacy of various CNN architectures on both preprocessed and raw EEG data for the purpose of sex classification and prediction. They did this using a dataset that contained children of both sexes. The sample population of toddlers contained both male and female children. Their research demonstrated that the same CNN architectures could achieve greater results with minimally preprocessed EEG data than with completely preprocessed EEG features [16]. This was demonstrated by the fact that the researchers were able to achieve the same level of success. This was shown by the fact that their findings showed that the same CNN architectures could produce better results. This was a demonstration of this point. Recent research [17] was conducted with the intention of investigating the possibility of forecasting drowsiness with the assistance of a single EEG channel and a convolutional neural network. This research was recently made public. (CNN).

According to the findings of our study, the accuracy of predictions and classifications made using raw EEG data is on par with, and in some cases even surpasses, that of the alternative method. Numerous studies have attempted to prepare EEG patterns for use in deep learning applications by employing discrete wavelet transforms (DWT) and fast Fourier transforms (FFT). These two types of transforms are often referred to as "discrete" and "fast," respectively. It is possible for the process to require a significant amount of trial and error when there is no universally accepted metric or spectrum of values to use when transforming the information contained in the brain signal. This is because the information contained in the neural signals is undergoing a transformation. Studies on brain signals that use DWT or FFT on the data collected can therefore generate findings that differ, albeit to different degrees. This is because the use of these techniques on the data collected is dependent on whether the study does or does not use them. The recommended framework calls for the use of the raw patient EEG data with only a minimal amount of preprocessing so that the full potential of deep learning architectures can be leveraged and EEG signals can be evaluated. This is necessary in order to fully leverage the potential of deep learning architectures.

4.2 DATASET

In this section, both the raw EEG data and any preprocessing processes that were carried out in order to achieve or standardize the beta frequency bands are addressed. These procedures were carried out in order to achieve the desired results. When talking about a collection of primary frequency bands, the frequency ranges delta, theta, alpha, beta, and gamma are the ones that are frequently brought up. Although the exact limits of these frequency bands change depending on the source, the frequency of delta brain waves is between 0.5 and 4 hertz (Hz). Delta brain waves have frequency ranges that can range anywhere from 0.5 to 4 Hz, and they are most prominent when a person is sleeping or dreaming. Theta brain waves have a frequency range of between four and eight hertz (Hz), and the most frequent time for people to experience them is when they are in an extremely deep state of exhaustion or sleepiness. Daydreaming and states of relaxed concentration are both correlated with the range of alpha brain waves that occurs between 8 and 12 hertz. When a person is anxious or very active, their brain waves will fluctuate between 12 and 35 hertz (Hz), a region known as the beta range. It is considered typical for the frequency to fall somewhere within this range. In conclusion, being in a state of intense concentration triggers the generation of gamma brain waves, which have a frequency that ranges from 35 to 50 hertz.

The EEG library that has been compiled by Temple University is quite comprehensive, and it can be utilized for deep learning research in the field of neuroscience. More than 30,000 EEG recordings spanning numerous generations of EEG recording equipment can be found in the current database. In addition, the database has information gathered from the brains of approximately 11,000 subjects between the years 2002 and the current day. This information was collected. The dataset includes both open-source European data format (EDF) files as well as text files comprising EEG reports that were made by neurologists during each EEG recording session. These neurologists made these reports while the subject was undergoing an EEG recording. The neurologists who were present for each EEG recording session compiled the EEG reports that are located in the text folders [23]. The full dataset comprises of female subjects, who account for 51% of the sample and range in age from less than a year to over 90 years old, with the average age being 51 years old. The subjects' ages can be found in the range of [and include] The ages of the participants range from well under one year to well over ninety years. The abnormal EEG corpus (TUAB), which is a collection of EEGs that have been characterized by a neurologist as either normal or atypical, is one of the many datasets that are included in the database. The database also contains a wide variety of other datasets. Artifacts of the electroencephalogram (EEG) such as eye movement, chewing, and shivering are generally recognized and labeled with the assistance of artifact corpora (TUAR), which are frequently used in classification efforts. The Temple University EEG seizure corpus, also known as TUSZ, is a collection of annotated EEG recordings that are derived from EEG signals and show locations at which seizures occurred. These recordings have the potential to be utilized in deep learning research for purposes including the identification of seizures.

The statistics required for this investigation came from the Abnormal Dataset, which is housed at Temple University. That dataset was supplied to the research team by Temple. (TUAB). However, the ultimate objective is to use raw EEG signals to predict the brain ages of individuals who have had a history of neurodegenerative diseases. The primary emphasis is on seizure patients because there is a high prevalence of individuals in the dataset who have a history of seizures. The TUAB dataset includes information that was collected from 564 individuals who either had seizures themselves or were evaluated for the possibility of having them. Readings taken from the electroencephalograms of people varying in age from 2 to 88 years old are included in the TUAB dataset. The participants whose EEG patterns were examined had, on average, 42 years under their belts when they took part in the study. (Figure 4.1).

Within the entirety of the data set, the age of 21 is mentioned a total of 24 times, making it the age category with the greatest frequency overall. In order to acquire the signal data, the universal 10/20 EEG node placement technique was employed. (Figure 4.2). Depending on how severe the patient's situation is, the length of time that these recordings are played back can range anywhere from thirty minutes to several days. The recordings will only run for a total of thirty minutes if the patient is being seen for the first time. 87% of the EEG signals were recorded at a frequency of 250 Hz, while the remaining data was sampled at 256 Hz, 400 Hz, or 512 Hz, as stated in the data information document from Temple University that can be located in the database. The data information document was retrieved from the database. This information was uncovered while searching through the database. Considering how essential it is to have a dataset that is appropriately homogenized, this is of the utmost importance. A second recording was necessary because this abnormal information was broken down into normal and atypical EEG readings, such as those with a high Theta frequency or slower wave activity. In order to eliminate the possibility of error brought about by either the recording instrument itself or the involvement of a human, these experiments make use of data obtained from the standard dataset.

In addition to the EEG recording EDF file that is kept for each patient, there are also instructional text files that are kept for that patient. The discrepancies in the transcripts are clarified by the information contained in these files. Each of these files contains information such as the date of the recording, general clinical information about the patient, whether they have a history of a particular disorder such as epilepsy or stroke, the patient's age, any medications prescribed that the patient had taken prior to the examination, and a neurologist's documentation regarding what was seen during the examination. Due to the fact that the sessions contain EEG recordings from various locations throughout the hospital [23], there are a great deal of different channel-recording configurations and channel labels that are utilized in order to characterize the EEG data. As a result of this, the results from the EEG can be characterized in a number of different ways.

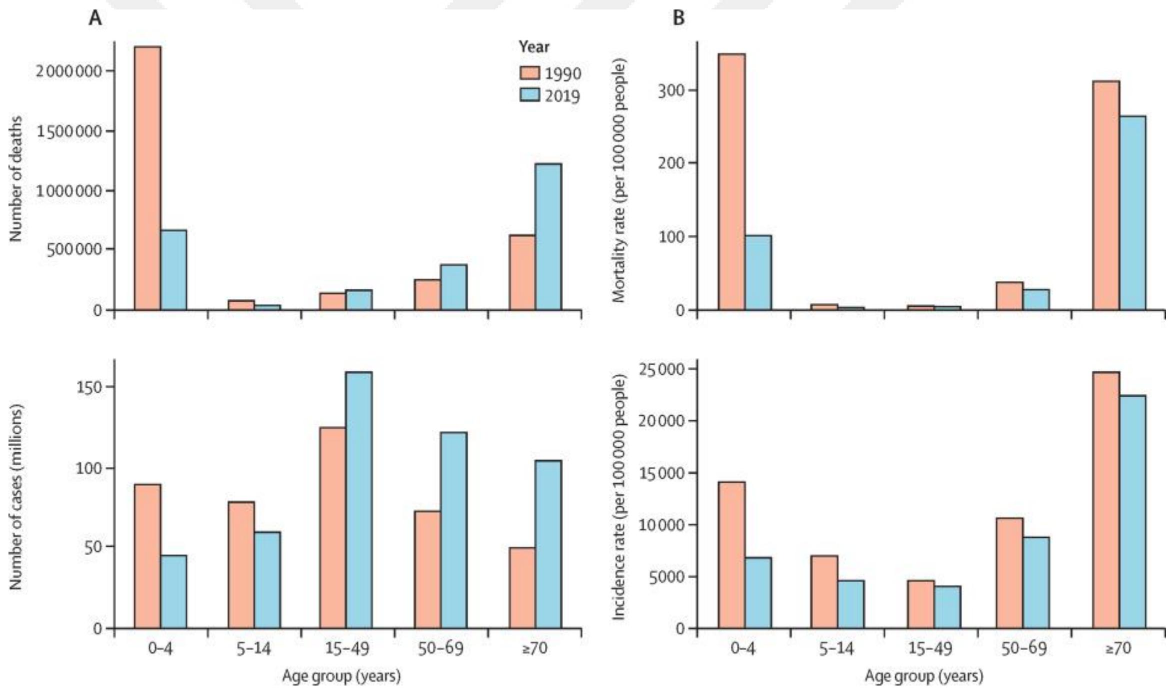

Figure 4.1: The Age Spread of the Patients in the TUAB Database.

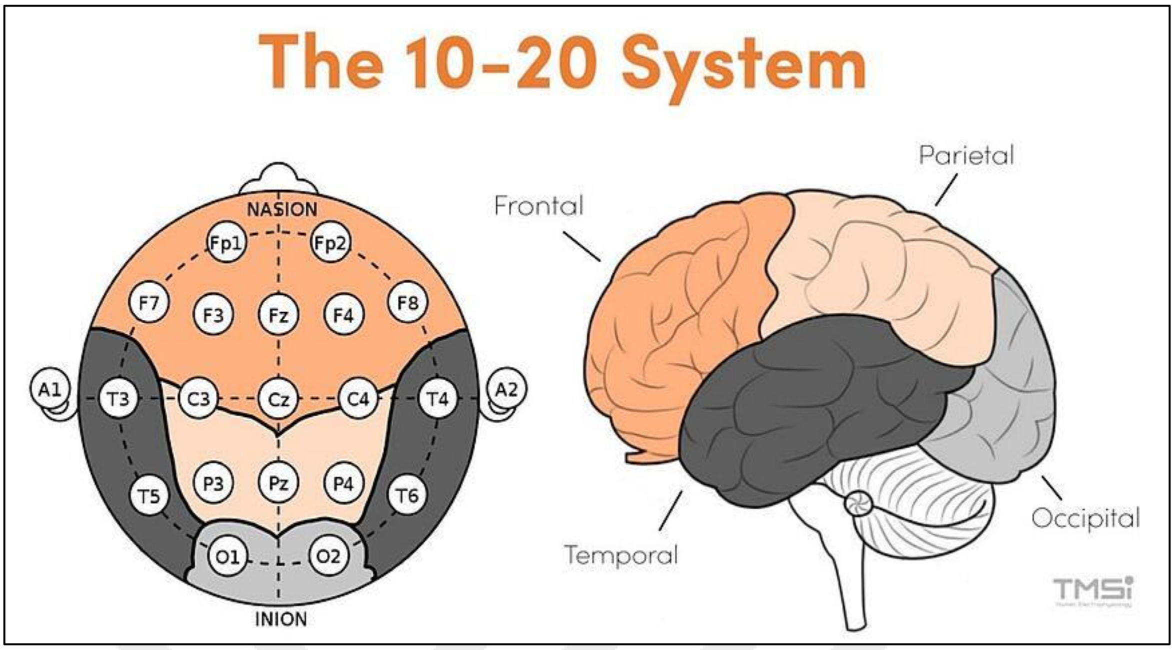

Figure 4.2: Fundamentals of the Worldwide Standard for EEG Electrode Placement: Both the 10/20 and 10/10 Systems.

4.3 EEG PREPROCESSINGS

Brainwaves from patients who have been diagnosed with the same condition as the model being taught are used when training deep learning models. A homogenized dataset with brainwave distributions that are consistent throughout can be obtained as a consequence of this process. According to the findings of the research, convulsions are to blame for 87 percent of all neurodegenerative diseases, whereas strokes are only to blame for 12 percent of these conditions. After the preprocessing of the EEG signals, the signals are then categorized according to the file name of the patient. After the patient's age has been extracted from the text files, either classification or regression can be used to make projections about the patient's future age.

Because the quality of the data that is being collected is such an essential factor in determining the quality of the data that is being used in any deep learning endeavor, this aspect of the data is taken into consideration at every stage of the process. It is common knowledge that EEG data are notoriously noisy and full of recording errors; consequently, it is an essential necessity to investigate the most efficient preprocessing techniques. When it comes to EEG signals, the frequency ranges that are of importance have been very precisely outlined. Figure 4.3 presents a flow chart representation of the technique that must be followed in order to prepare raw EEG signals.

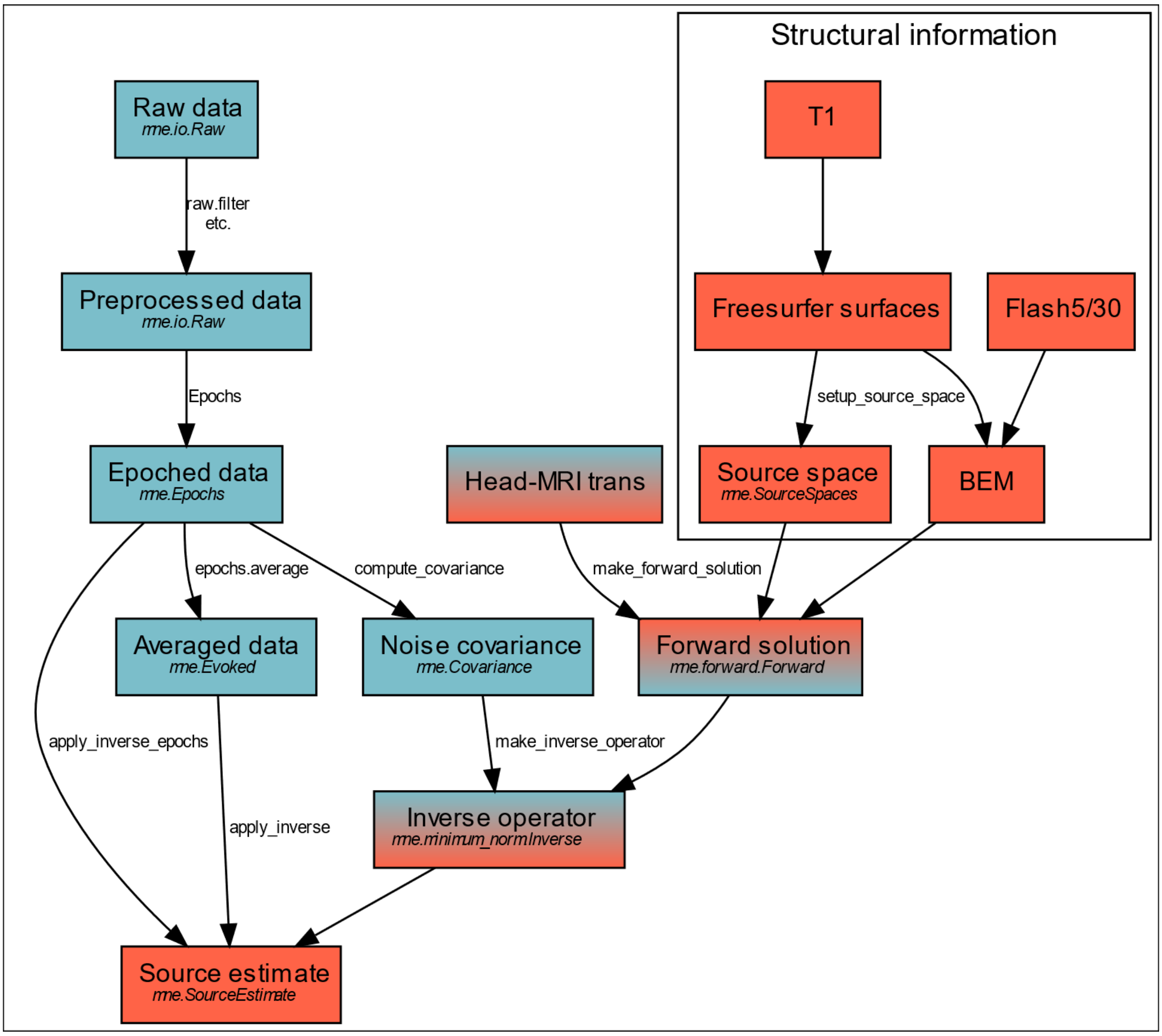

Figure 4.3: EEG Pre-Processing Flowchart.

After the first minute and a half of collecting electroencephalogram (EEG) signals, the data is broken up into eight-minute segments. This is done in preparation for age prediction and classification, which are the two primary objectives of this research. Those goals are age prediction and classification. This is done so that any preprocessing methods will not be hindered by significant spikes in data during the first few minutes of recording, and also so that there will be no space for human error at the beginning of the process. Both of these goals are accomplished by performing these actions. (Figure 4.4). Following the recording of the EEG signals, they are bandpass-filtered using a low pass filter with a frequency of

120 Hz and a high pass filter with a frequency of 0.5 Hz. It is the job of the high pass filter to get rid of any artifacts at the lower frequencies, and it is the job of the low pass filter to get rid of any inconsistencies at the higher frequencies. Since 87% of the data in the dataset were recorded at 250 Hz, but some files were recorded at much higher frequencies, the next stage in order to generate a completely homogenized dataset is to resample the EEG recordings to 250 Hz. This is because some files were recorded at much higher frequencies. This is essential due to the fact that certain files were recorded at significantly greater frequencies.

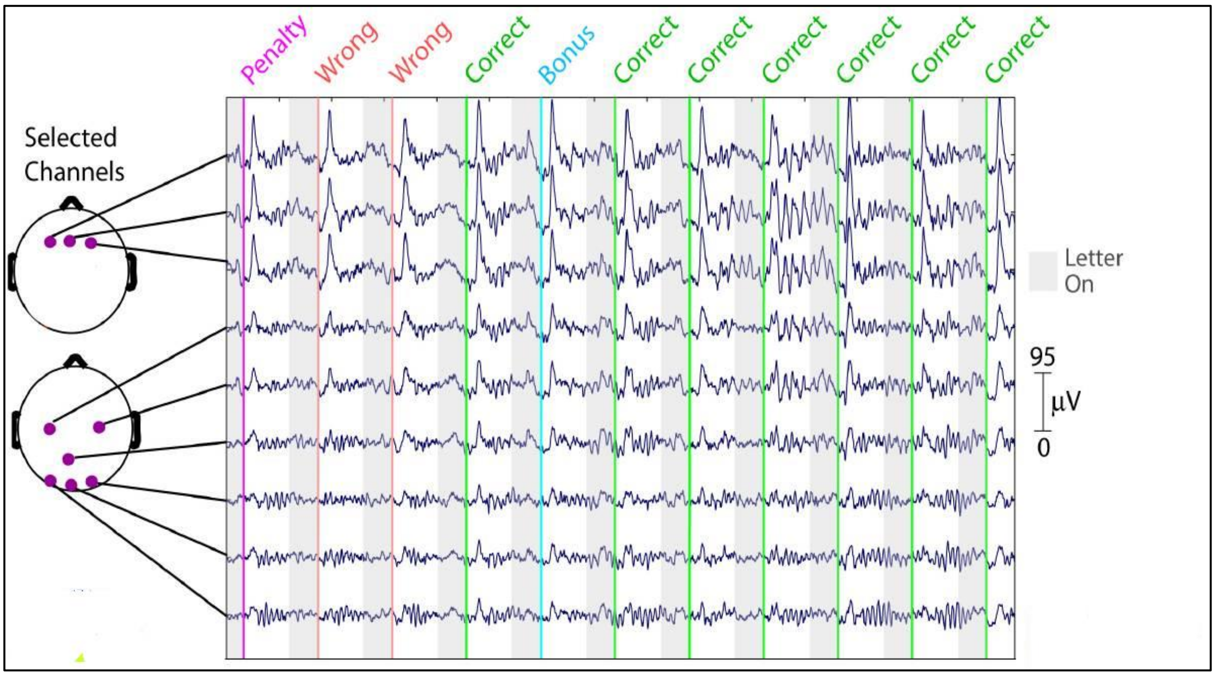

Figure 4.4: The Original Representation of the EEG Data.

Several different illustrations are used to depict the procedure as it is being carried out. Figure 4 demonstrates the recovery of raw EEG recordings from the EDF files, and Figure 4.5 displays the same man's EEG recordings from the dataset after they have been compressed, filtered, and resampled. Both figures pertain to the same 34-year-old individual. Both of these figures originate from the same underlying information. Each of the EEG recording locations that were a part of the collection can be represented by their own unique line that illustrates how their microvolt-scale signal changed over the course of time. As can be seen in Figure 4.4, the large, almost flatlined recordings of EEG signals needed to be removed in order to guarantee that they would not impede the subsequent processing of the data. As a direct consequence of this, the recording time had to be broken up into segments of eight minutes each, beginning with the first sixty seconds of the recording. During the first minute and a half of an EEG recording, the signals typically stabilize into what could be considered a normal EEG recording. After this point, the recording continues as normal. These gigantic recordings that are flatlined usually show up during the first minute and a half of an EEG recording. Such recording blocks are a subject of debate with respect to their origin, as they could originate from human error when setting the EEG points on the subject's scalp, the subject having their eyes provide to stimuli in the initial stages of recording, or simply as a byproduct of the recording mechanism. Figure 4.5 displays recordings of the signals after they were processed by the original resampling and cropping, which resulted in a more conventional EEG recording. These processing steps are shown after the signals were subjected to them.

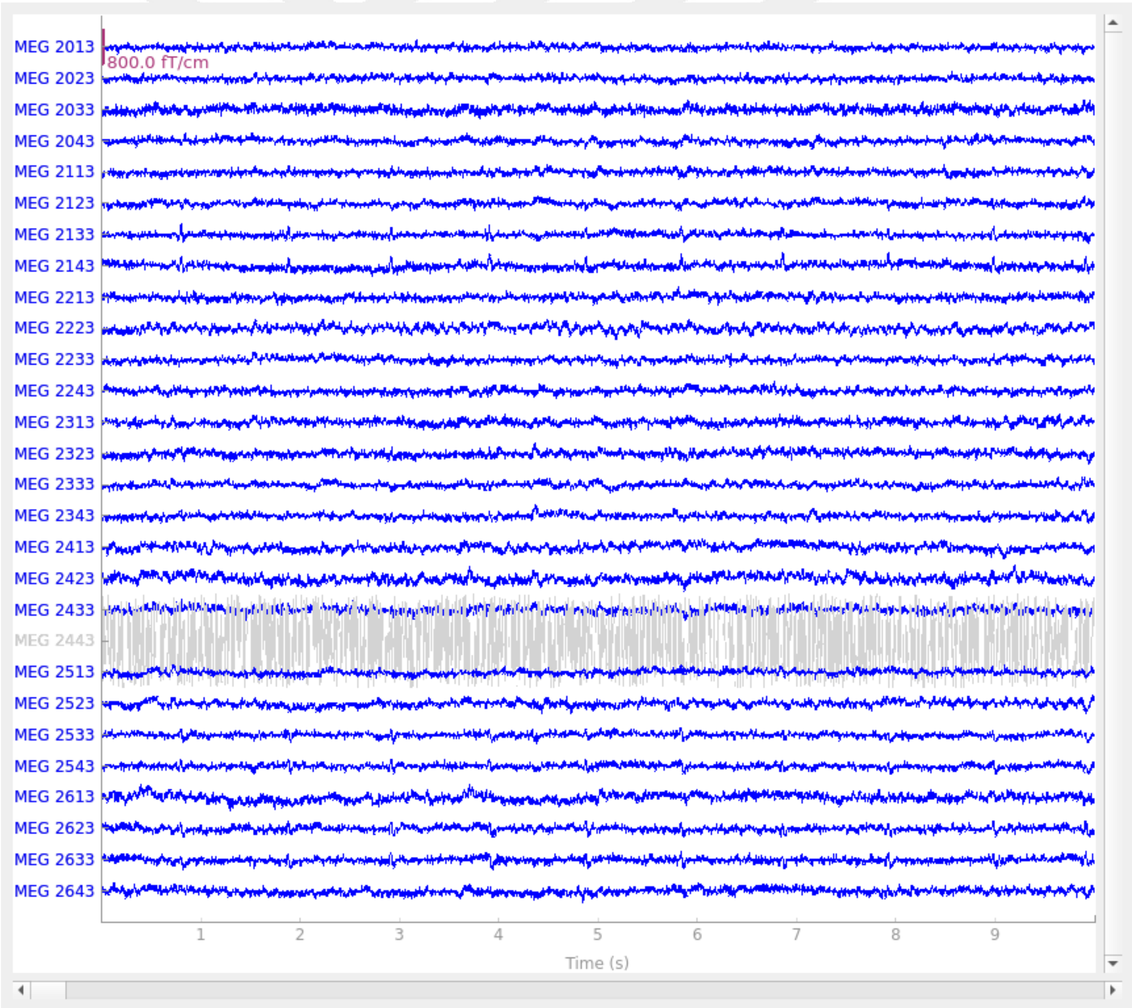

Figure 4.5: The EEG Data was Resampled and Re-Visualized After Being Cropped.

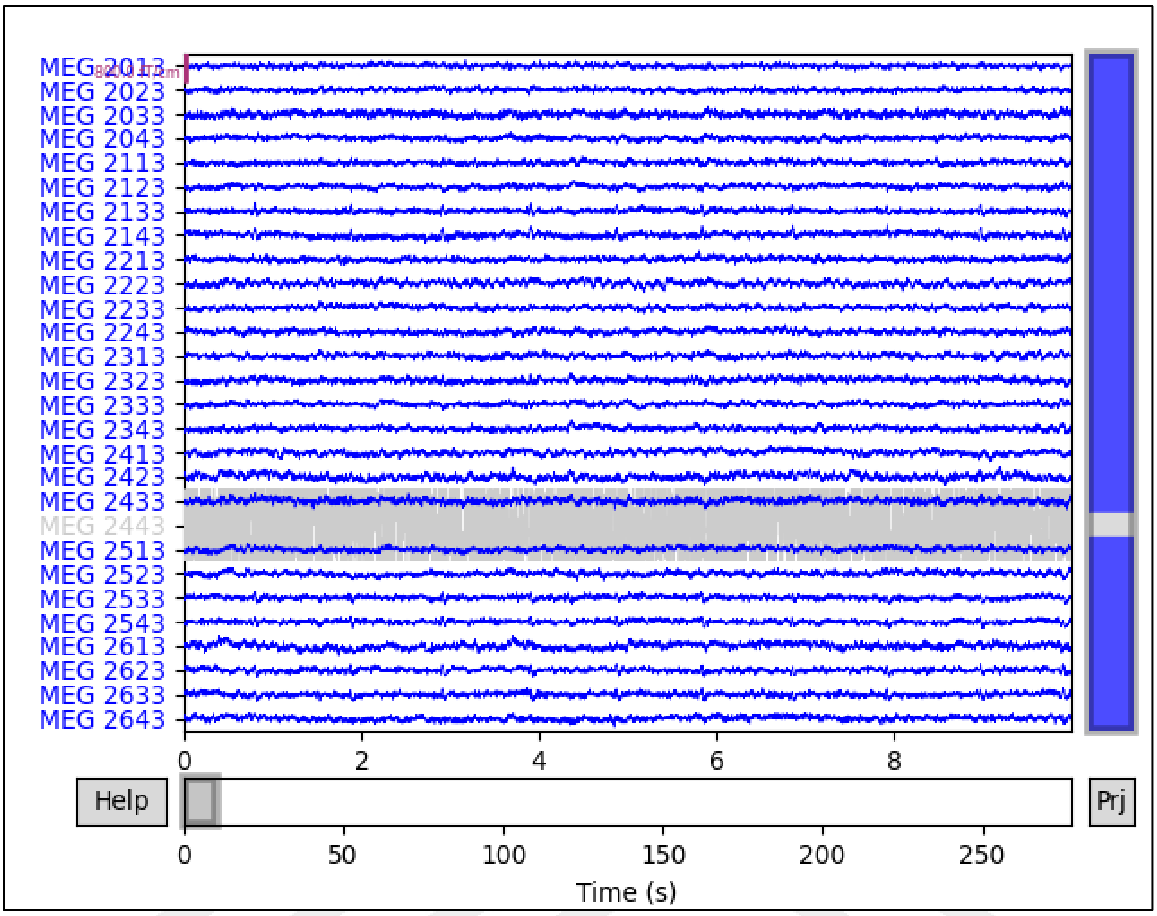

Figure 4.6: The Development of Documenting Intervals of Three Seconds.

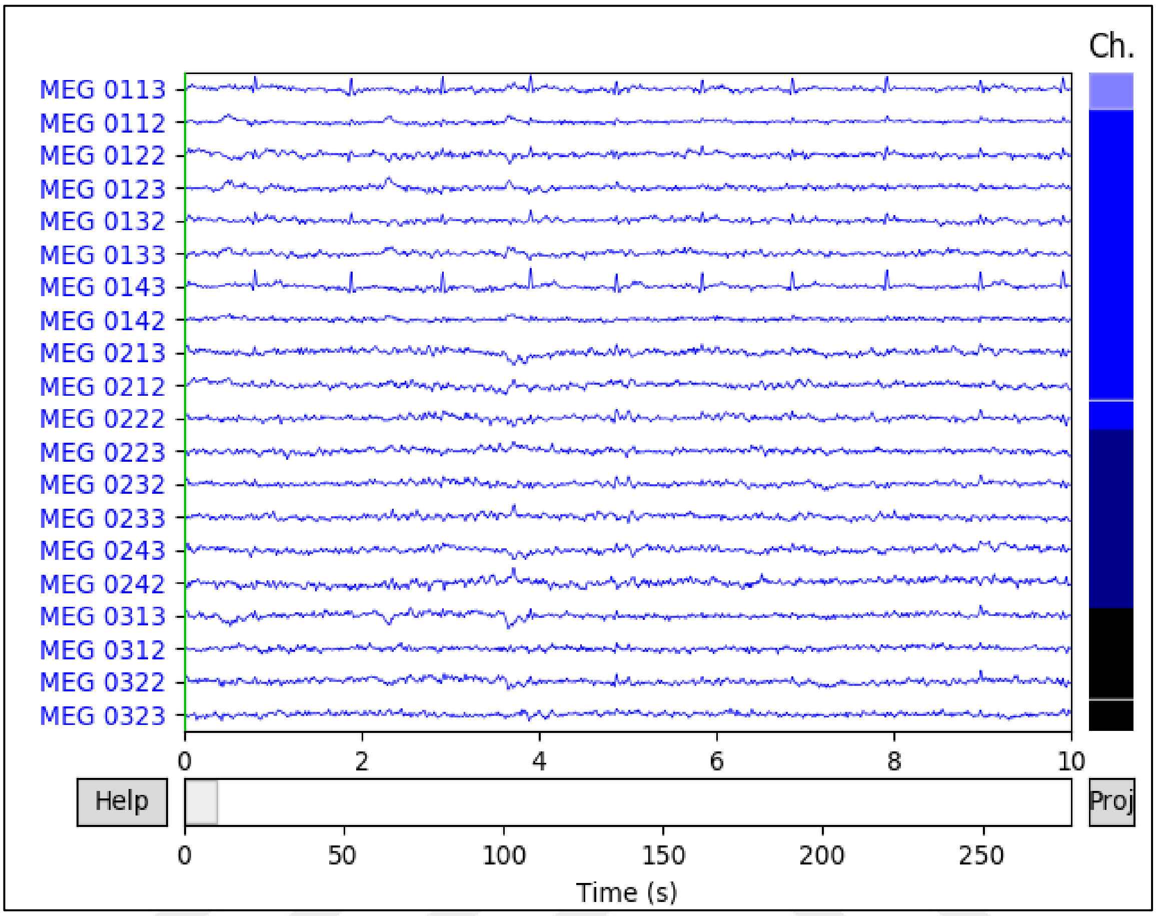

Figure 4.7: Elimination of EEGs Recorded After a Bad Era.

In specific situations, preprocessing is carried out in order to standardize the output data while testing is being carried out. This may be the case in a variety of contexts. This contributes to the narrowing of the variety of numbers that are produced by the filters. The freshly obtained knowledge is applied to the examination of the EEG signals before any processing has been done to them. This is done after the inaccurate time intervals have been eliminated from consideration. The reasoning behind this procedure is based on testing the ability of the deep learning Designs to extract features and detect develops in the raw data and make comparisons between more significantly accepted preprocessing techniques and the more fresh increased popularity of using of completely learning recurrent neural networks.

Either method could be used to examine each data file that includes information about a particular neurodegenerative disease; however, the one that is actually used will be determined by the preprocessing strategy that is being evaluated. Both methods have their advantages and disadvantages. The gathered data points are written down into a standardized CSV file in order to make the process of training and evaluating the four different deep learning models as straightforward as possible. The freshly generated CSV files start with an inventory of patient file information, then move on to preprocessed or raw data, and finally, patient age information that was extracted from the clinical text file and stored in either a categorized or raw state depending on which state it was in when it was extracted. In order to facilitate the development of the qualitative aspect of the projection, the ages of the patients whose information is contained in the collection are categorized according to a number of different age ranges.

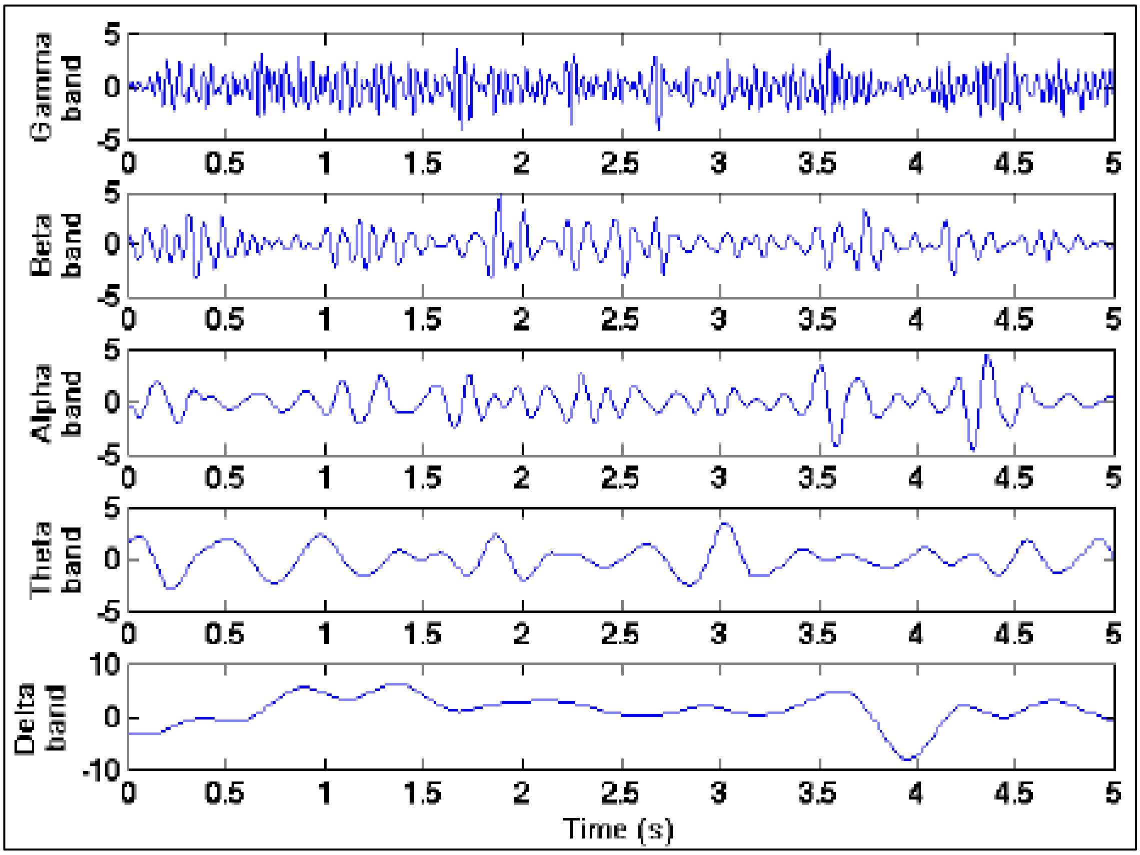

Figure 4.8: Extraction of Different Frequency Ranges.

4.4 AGE RANGES

Because the patient data include a broad range of ages, it is recommended that the potential consequences of the model, as well as the data used for building the model, be restricted.

Both the patient age classifications and the actual ages of the patients are taken into consideration when evaluating the two distinct kinds of model outcomes.

Table 4.1 presents the initial grouping of patients into age categories that were considered appropriate. These age categories encompass the entire age continuum, from neonates to the geriatric population, with a predominant focus on the earliest and latest phases of brain development, respectively. This includes people of all ages, from newborns to the elderly. Patients who are between the ages of 30 and 50 are given an initial degree of treatment that is lesser than that given to patients who are between the ages of 18 and 29 or over the age of 60. This is due to the greater age difference that occurs between these groups. As a result of the fact that their primary brain development is finished by the time they are in their mid-thirties, individuals in this age range are particularly susceptible to the neurological issues that are typical in toddlers and the elderly. On the other hand, in order to produce a collection that is more representative of the population as a whole, we use people who are at least 30 years old. (Table 4.1). 32% of the patients in the aberrant EEG sample who had an indication of epilepsy or seizures in the past were three hundred and five years old or older. These patients had all been diagnosed with epilepsy or seizures in the past. (Table 4.1). Data from patients aged 90 and later are included in the dataset that was collected by the Temple University EEG Corpus; however, these data constitute only a minute fraction of the complete collection and should not impact the standardization of the dataset. The dataset was collected by the Temple University EEG Corpus. The problem changes from one of classification to one of regression analysis, with the objective of forecasting the ages of the patients in years, as the original ages of the patients are also used for training and assessment. Because of this, the issue is no longer one of classification.

Table 4.1: Initial Patient Age Ranges.

Age Range	Approximate Percentage of Dataset
$7-11$	2%
$13-16$	0%
$17-24$	12%
$25-30$	11%
$32-47$	32%
$47-56$	24%
$57-61$	7%
$65+$	13%

4.5 CONVOLUTIONAL NEURAL NETWORKS

The Convolutional Neural Network is yet another prevalent and widely used architecture for a deep learning network that discovers widespread application in classification-related tasks. (CNN). Convolutional layers, pooling layers, activation layers, and completely connected layers are the standard components that go into the construction of a CNN [20]. These four layers are referred to as the standard components that make up the construction of a CNN. CNNs are ideal for end-to-end learning, which refers to the process of learning from raw data without the use of features to guide the process. This is due to the fact that the objective of studying the hierarchical structures that are inherently present in natural signals is to gain knowledge from the unprocessed data without making any feature selections. CNN's most significant flaw is that it frequently and with a high degree of confidence makes projections that turn out to be incorrect. This is by far the network's biggest shortcoming. Additionally, convolutional neural networks (CNNs) might call for a sizeable amount of training data and might require a noticeably lengthier period of time to learn than models with a lower level of complexity [20].

In recent years, CNNs have become a substantially more prevalent instrument for evaluating the data from EEG patterns, in comparison to RNNs, which were previously the predominant method. The Shallow Filter Bank Common Spatial Pattern Network (SFBCSPN), which was developed by Schirrmeister [20], is used as a guideline, whereas the SFBCSPN [19] is used for determining the age of an individual based on their EEG. Both of these networks were created by Schirrmeister.

In contrast to what Engemann did, the approach that we are going to go over here does not require any phases that are considered to be preliminary. The writers of [19] standardize the neuroimaging data after first converting the EEG waveforms into the Brain-Imaging Data Structure (BIDS) format. The data is bandpass-filtered between 0.1 and 49 Hz first, and then it is divided into 10-second epochs that correspond with the eyes-closed and eyes-open resting-state periods. Finally, the data is presented in a tabular format. This makes it possible to conduct a more in-depth analysis of the material. After capture, amplitudes of EEG impulses that have been captured are quickly filtered out using a screening algorithm. To ensure that the data is not inconsistent in any way, the original sampling rate of 21 channels in TUAB is increased to a frequency of 200 Hz, and then the information is resampled. Because we want to keep things as simple as possible, we only use the very first sample that we collect from each person. After the incident, the data that had already been collected was resampled so that the performance of the deep learning CNN could be evaluated. When determining the efficiency of our deep learning recurrent neural network designs, we make use of the model described in [19] and the MAE number that it supplies, which is 8 years. Additionally, we take into account the results of our previous experiments. When compared head-to-head with the other available choices, the method that comes recommended by our team has an MAE number of 7 years.

5. RESULTS AND DISCUSSION

In this section, we will present the general findings from our investigation of the models, as well as the parameters that were utilized in the ordering of these results. Additionally, we will discuss why these results were ordered in the manner that they were. Table 4.1 contains a listing of the ages of the individuals whose EEG data were used from the TUAB Corpus. You can view this listing here. The remaining ten percent of the dataset was used as a confirmation set, and while the model was being trained on it, its inputs and outputs were divided in a ratio of 70:20. According to this, there are 279 EEG samples that are used as part of the training collection. In order to evaluate the efficacy of the model, a total of seventy-eight EEG measurements were utilized. There are a total of 31 EEGs that are being utilized for the verification process at this time.

Because the model-checkpointing evaluation takes into account both a slowdown of the learning rate and an early stopping, each of the models is taught at a different pace in order to make up for the fact that the evaluation takes into account both of these factors. A decreasing learning rate is initiated and kept going in order to stop the process of training from reaching a stopping local minimum. This is done both automatically and manually. The condition that will be activated is the learning rate reduction condition if the validation loss is kept at the same amount for five repetitions in a row. If the model does not show any signs of development after being trained for five epochs, the learning rate will be cut in half as a corrective measure. Because of this decrease in learning rate, an absolute maximum of 5 x 107 pieces of information are lost. The construction of the model determines the optimal group number, which is then fine-tuned in order to raise the model's performance to its maximum possible level. The models' loss functions are also modified appropriately in response to the findings of the investigation. As precision measures, the mean squared error, root mean squared error, and the mean absolute error are employed when working with data that consists of actual patient ages from individuals as a regression problem. When categorical patient ages are used, categorical cross-entropy is evaluated as a loss function, and categorical accuracy is used to determine precision. [Case in point:] [Case in point:] [Case in point:] [Case Both of these ideas are connected to the concept of accurate categorization. In the following paragraph, we will explore even deeper into this subject, and in the following section, we will address these measures in greater detail.

When age categories are used, a one-hot encoding of patient ages into vectors can be achieved by utilizing label encoding in combination with classification. This will allow for a more accurate representation of the patient population. During the process of one-hot encoding, each distinct numerical value is assigned its very own representation in the form of a binary variable. Subsequently, this variable is taken out of the equation when it comes time to encode the labels. The following is an illustration of what a one-hot-encoded graphic for people between the ages of 41 and 45 might look like: [0, 0, 1, 0, 0, 0]. They would fall into the third age classification grouping as a result of this fact.

Throughout the course of this investigation, numerous iterations of the offered models have been put through their tests. The models that proved to be the most successful in terms of producing desirable outcomes will be dissected in the succeeding portions of this report. The loss and precision measurements that were recorded over time as training progressed on the training and evaluation sets of EEG data, respectively, are represented in Figures 5.1 and 5.2, respectively. These figures are displayed on the respective sets of data. compares the mean age of the actual testing data to the mean age that was forecasted by each deep learning model during the regression analysis instances. This helps to demonstrate the error margins associated with the mean age prediction. The category accuracy percentage for age categorization is presented in Table 5.1, and Table 5.2 provides the findings for precision, recall, and the F1 model. Both figures are included in this section.

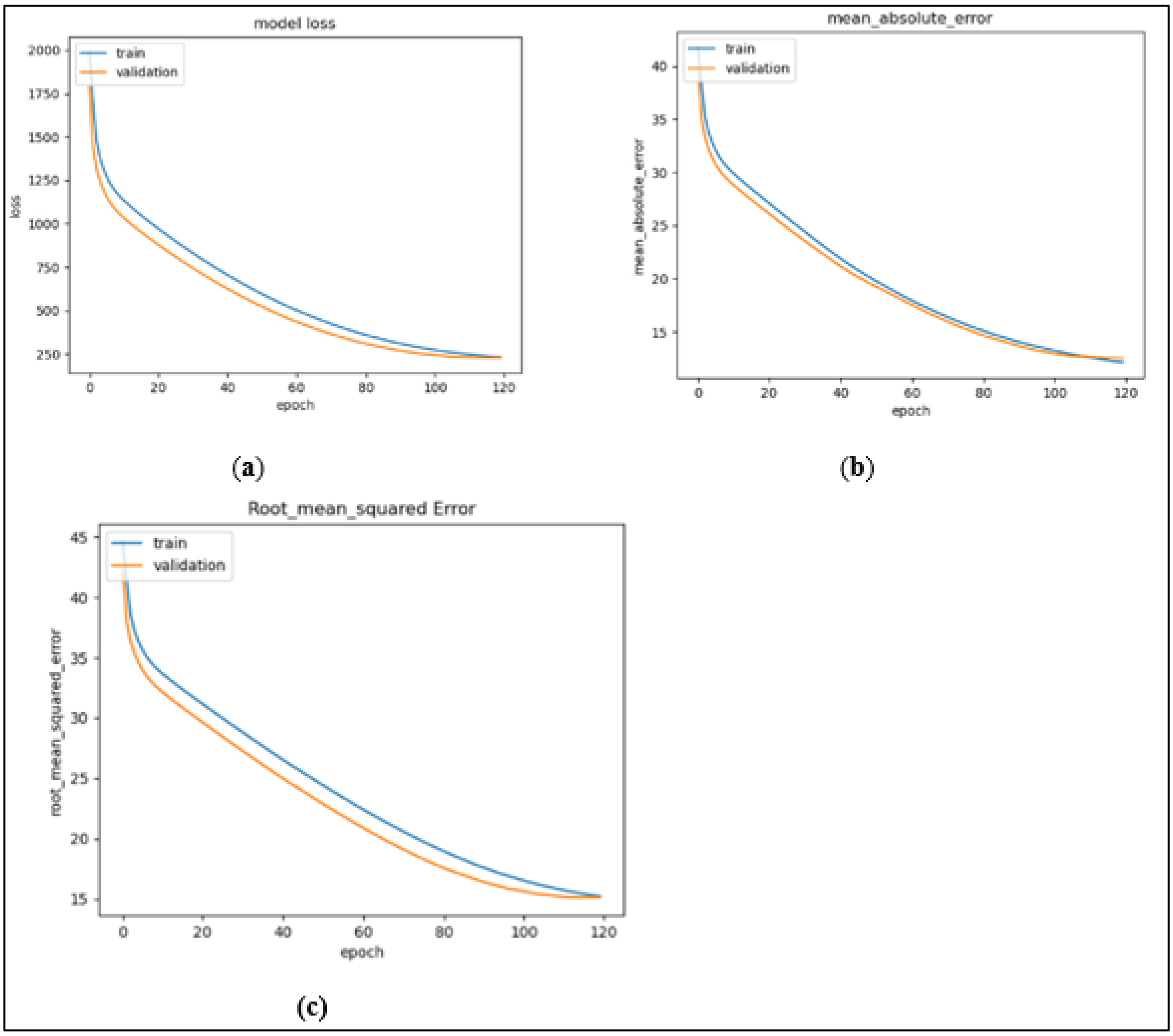

Figure 5.1: Loss (MSE) of an LSTM Trained on EEG Data Using Regression Analysis (A); Mean Absolute Error (MAE) of an LSTM Trained on Raw EEG Data Using Regression Analysis (B); Root Mean Squared Error (RMSE) of an LSTM Trained on Raw EEG Data Using Regression Analysis (c).

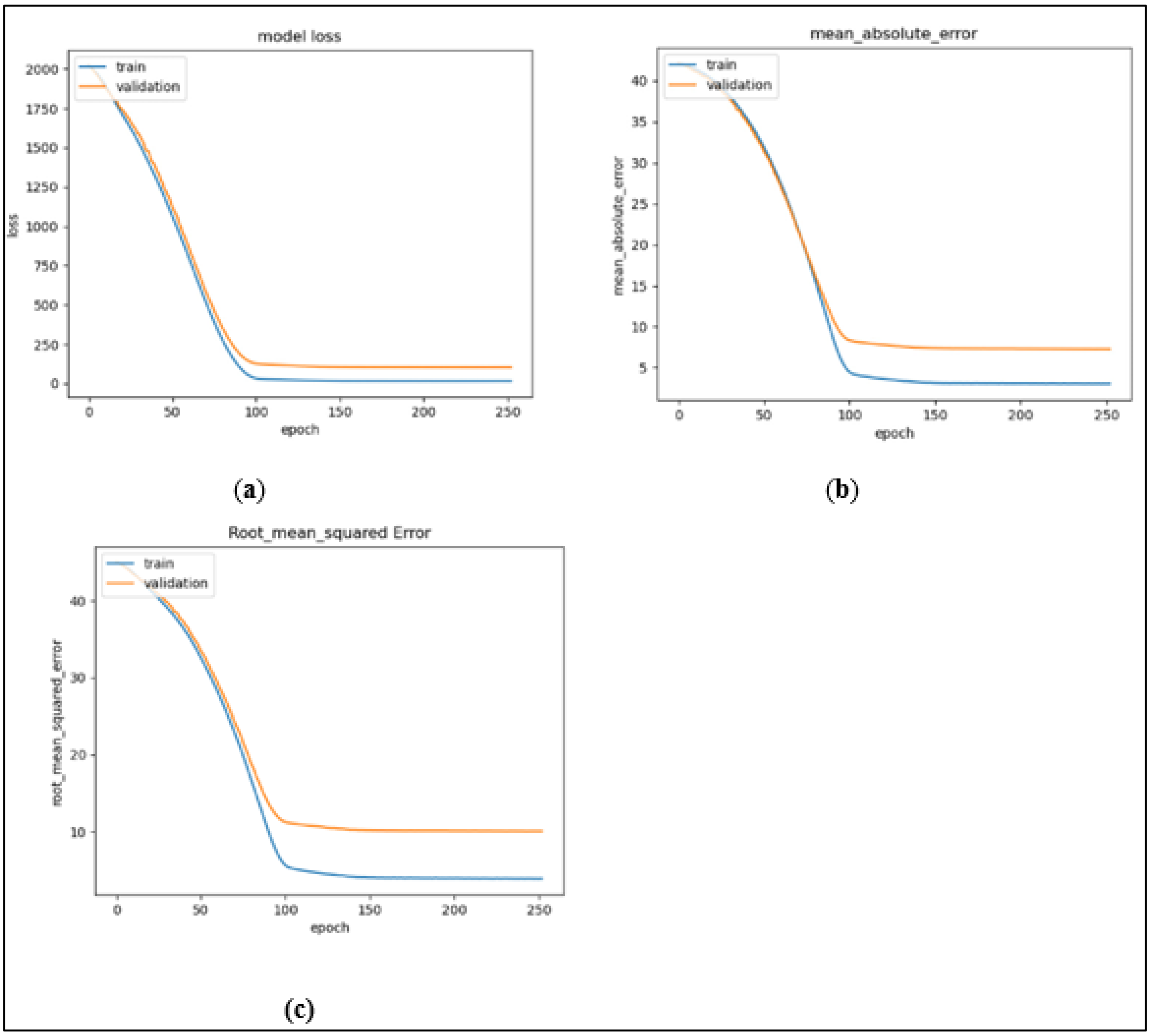

Figure 5.2: The Following Metrics Measure the Efficacy of BLSTM Models: (A) the Loss (MSE) of a BLSTM Model Trained on Raw EEG Data with Regression Analysis; (B) the Mean Absolute Error (MAE) of a BLSTM Model Trained on Raw EEG Data with Regression Analysis; and (C) the Root Mean Squared Error (RMSE).

Table 5.1: Results of Each Model From Regression Analysis.

	MAE	**RMSE**
LSTM	12.5	15.1
GRU	12.2	14.8
BLSTM	7.3	10.07
BGRU	6.5	9.1

	Train	Valid	Test	Recall	Precis	F1 Score
BLSTM	99%	91%	90%	0.9	0.9	0.9
BGRU	99%	93%	93%	0.93	0.92	0.93

5.1 EVALUATION METRICS

The mean squared error for the loss, the mean absolute error, and the root mean square error for the accuracy measure are used to assess the models in a regression analysis performed on the raw patient ages. Metrics such as categorical-cross entropy loss and categorical accuracy are applied to the task of patient age range categorization.

5.2 CLASSIFICATION METRICS

When evaluating multiclass categorization issues, the most prevalent loss function is the categorical-cross entropy. Categorical information is defined as "observations y" where y can only take values from a set of K discrete components represented by K one-hot vectors. Under a category distribution with parameter, the cross-entropy loss is equal to the negative log-likelihood of y >=. The value of cross-entropy is represented by the function.

$$(\pi; y) = -\sum_{k=1}^{K} y_k \log \pi_k \Leftrightarrow p(y; \pi) = \prod_{k=1}^{K} \pi_k^{yk} \quad (5.1)$$

One consistent probability model for discontinuous data over K classes is defined by cross-entropy loss.

The confusion matrix is used to characterize the generalizability of the age categorization models on the testing data sample, and is the last measure used in the assessment process. In order to assess a classifier's performance, a confusion matrix is frequently employed.

Precision, recall, and F1-score are three additional measures used to assess a classifier's efficacy. To determine recall, use Equation (5.2), which is the percentage of properly recognized favorable inputs:

$$\text{Recall} = \frac{TN}{FP + TN} \qquad (5.2)$$

In Equation, precision is defined as the fraction of true positives anticipated by the classification (5.3):

$$\text{Precis} = \frac{TN}{FN + TN} \qquad (5.3)$$

The test's accuracy, as determined by a weighted sum of precision and memory, is indicated by the F1 result. One is the best possible F1 result, while zero is the worst. As shown in Equation (5.5):

$$\text{F1} = \frac{2x\ Precis\ x\ Recall}{Precis + Recall} \qquad (5.5)$$

When employing the matrix, one can determine the usefulness of a classification by inspecting the memory, precision, and F1 evaluations that are generated as a direct consequence of employing the matrix [32].

The receiver operating characteristic (ROC) graph is an additional method that can be applied in order to assess the degree of precision that a classification system possesses. This method can be used in order to evaluate the accuracy of the system. The ROC curve is a form of histogram that presents memory and false positive rates at a variety of different classification levels. These rates can be viewed at any point along the curve. It is intended to demonstrate how beneficial a categorization model is, which is its primary purpose. An evaluation of the receiver operating characteristic (ROC) curve can be carried out utilizing a sorting-based methodology called the area under the receiver operating characteristic curve. (AUC). The area under the curve (AUC) is a comprehensive effectiveness predictor due to the fact that it takes into consideration all of the different cutoffs that are used for classification. The area under the curve, also known as AUC, is a measurement that demonstrates how likely it is that the algorithm will unilaterally designate a greater score to a positive instance as opposed to a negative example. The level of probability is represented here as a proportion. The area under the curve (AUC), which is concerned less with the exactitude of the numbers that are generated and more with the consistency with which the findings are displayed, is used to evaluate the precision of the predictions that are generated by a deep learning model. This evaluation takes place with the help of the area under the curve. The AUC can be given any value between 0 and 1, with 0 indicating a test that is completely inaccurate and 1 indicating a test that is completely accurate. The AUC can be allocated any number between 0 and 1. If the threshold number is set at 0.5, then it indicates that the findings of the test cannot be used to accurately categorize any of the age categories. This is the case regardless of which age group is being considered. If the area under the receiver operating characteristic (ROC) curve for a patient descends above the straight line that is presented in the presentation of ROC curve diagrams, which symbolizes the requirement for the deep learning model's distinguishing ability, then the ability to determine a patient's brain age has improved. This would lead one to believe that a more precise estimation of the patient's cortical age is possible.

5.3 EXPERIMENTAL RESULTS

Categorization analysis seeks to make projections pertaining to particular classifications as opposed to endeavoring to forecast a general pattern based on the data that is examined. Table 5.2 displays the age distributions of the individuals who have been surveyed. In spite of the overall decrease in the number of examples, the dataset that is generated will have a more consistent distribution, which is important when constructing a model for categorization. This will be the case despite the fact that the overall number of instances will decrease. However, in order to produce a collection that is representative of the population as a whole, the categories that appear less frequently than the age group that is encountered the most frequently are oversampled. This is done in order to produce a collection that accurately reflects the demographics of the entire population. Before obtaining classification results, it is essential to first standardize the patient age categories into one-hot vectors. Only then can the results of classification be obtained. In contrast to the single node that was used for the regression analysis, the output dense layers of these models each have six nodes, one of which corresponds to each of the classes. Previously, only a single node had been used. The BLSTM model that was used in this investigation obtained validation accuracy of 91% after 35 epochs of training, with F1 and precision values of 0.9. This was accomplished with both F1 and precision values being 0.9. The utilization of the identical hyperparameters as in earlier investigations resulted in the successful completion of this task. In spite of the fact that there is a propensity for models to be overfit to the training dataset, as shown by the diagrams in Figure 5.3, there is no perceptible increase in the amount of precision loss either during training or later in the process. This is the case even though there is a tendency for models to be overfit to the training dataset. Figure 5.3a illustrates the model loss, and Figure 5.3b demonstrates the model's precision. Both figures can be found in the same file. Both numbers are listed down here for your convenience. This overfitting may have happened because the regularization and generalization approaches, dropout, and group normalization that are typically used to combat overfitting were not activated in the testing process with the validation set. Another possible explanation is that the validation set was not large enough. In addition to this, the validation collection may not have been used, which may have contributed to the overfitting that happened. The ROC curves for the BLSTM model that was used are depicted in Figure 5.4 a,b, with a zoomed-in look of the region between a false positive rate of 0 and 0.3 displayed in Figure 5.4b. Figure 5.4a shows the ROC curves for the model. The statistics were analyzed with the help of this algorithm. The production of AUC values that are consistently in the upper 90% demonstrates that the BLSTM model does an excellent job of classifying individuals into one of the six age categories. This is demonstrated by the numbers presented here. The BLSTM algorithm that is used has a high degree of precision for individuals aged 61 and later; however, when it comes to individuals aged 30 to 40, it has significant difficulties. This is because elderly individuals have a higher risk of cardiovascular disease. Figure 5.5a and b illustrate the ROC graphs that represent the BGRU's performance. These graphs demonstrate the model's slightly superior discernment ability, specifically when it comes to categorizing individuals in the younger age category of 30-40 years old. In particular, the model performs slightly better at classifying individuals in the younger age category.

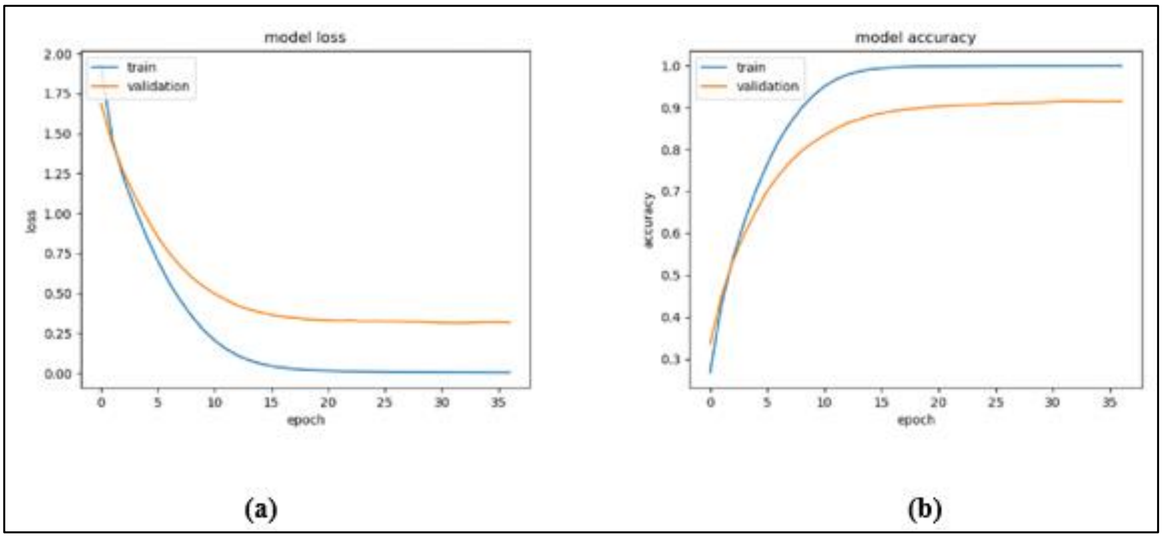

Figure 5.3: Categorical Cross-Entropy Loss of the Used BLSTM Model on the Raw EEG Data (A) and Categorical Precision of the Used BLSTM Model on the Raw EEG Data (B) are Two Measures of the BLSTM Model's Performance.

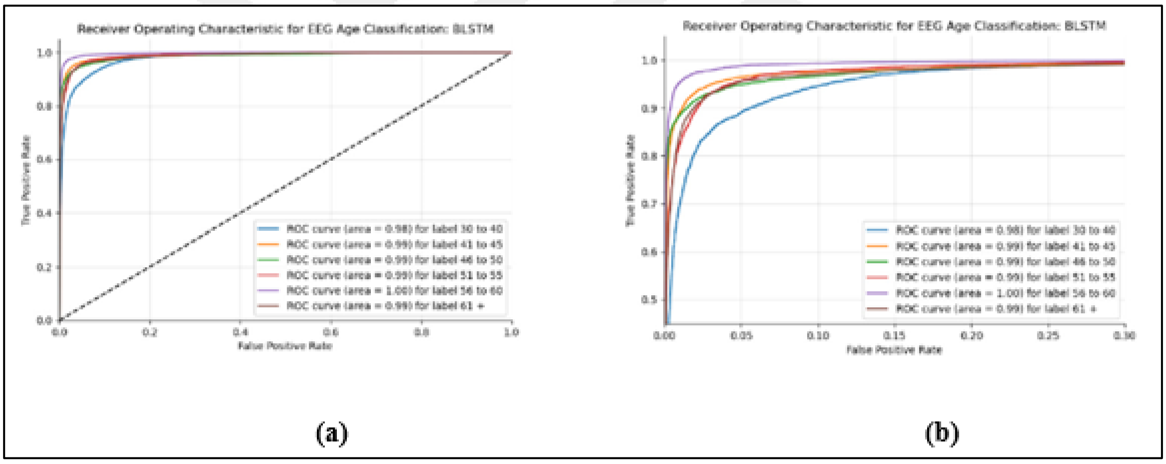

Figure 5.4: Reciprocal Operating Characteristic (ROC) of the Used BLSTM Model on the Unprocessed EEG Data: Images: (A) Complete ROC Diagram; (B) a Magnified Section Showing the Introductory Features of the Experiment.

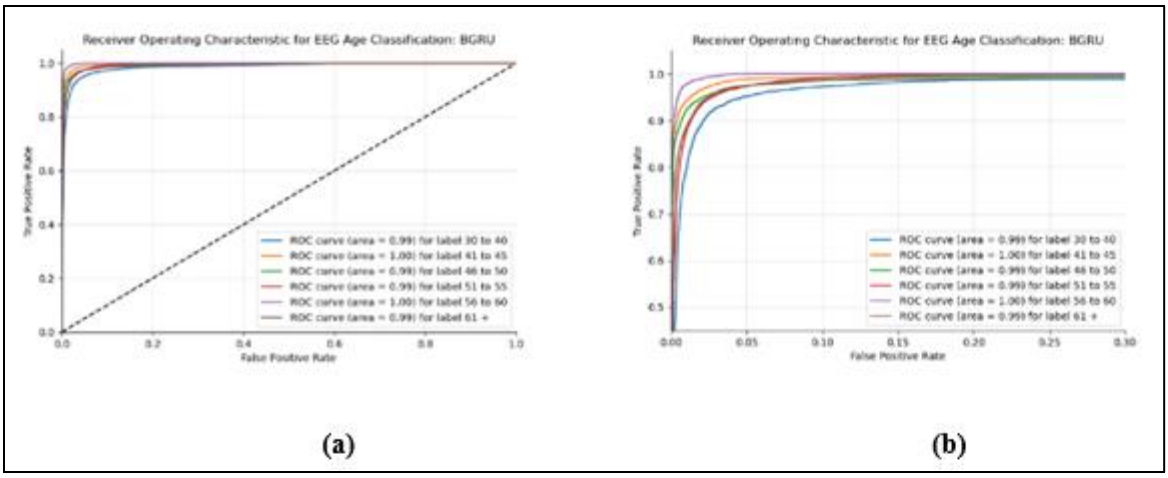

Figure 5.5: Recovery of Raw EEG Data Using the Applied BGRU Model: Images: (A) Complete ROC Diagram; (B) a Magnified Section Showing the Introductory Features of the Experiment.

On the test data set, the suggested design obtains an accuracy of 90% (range: 80% - 95%) when classifying patients' brain ages. (Shown in Figure 5.6).

Figure 5.6b displays the BGRU's findings, which are marginally more accurate (93%), with F1 and precision values of 0.93 and 0.92 (also displayed in Figure 6.7b).

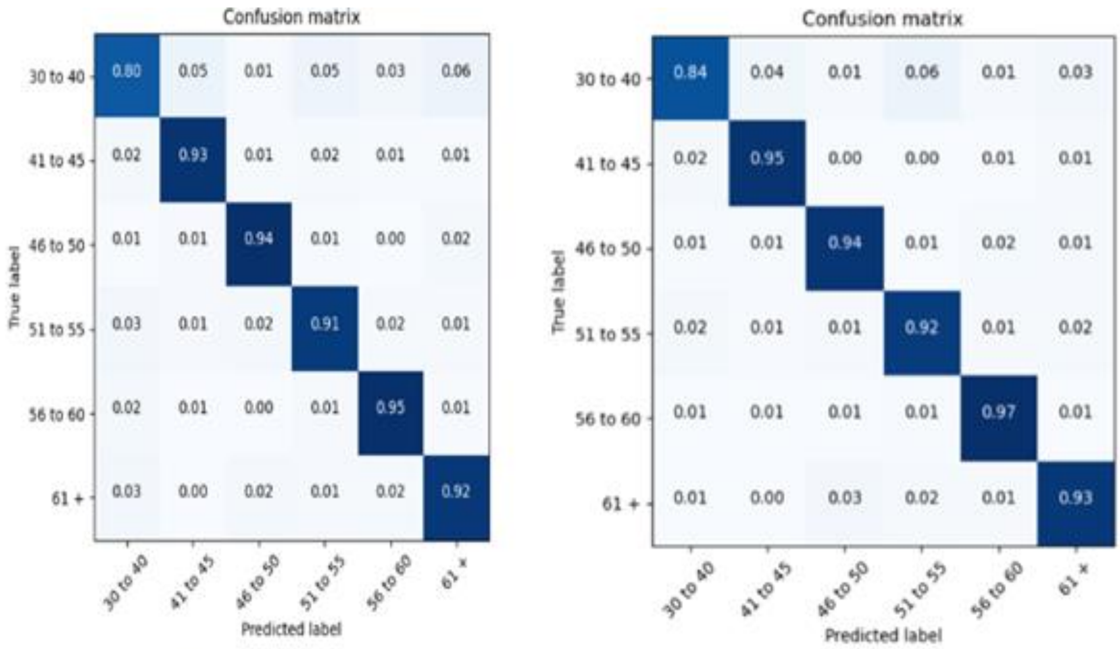

(a) (b)

Figure 5.6: Disordered Matrix Originating from (A) BLSTM raw Data Testing and (B) BGRU raw Data Testing.

6. CONCLUSION AND FUTURE WORK

Electroencephalography is one approach that can be utilized in the evaluation of neuronal activity. This technique records the electrical activity that occurs within the brain. Patients who suffer from epileptic convulsions or brain damage as a result of a stroke are among those who stand to benefit the most from EEG monitoring as a result of the continuous record of the electrical activity in their brain. This is one of the reasons why electroencephalograms (EEGs) are becoming increasingly popular. People who live longer are at a greater risk of developing neurodegenerative diseases like Alzheimer's disease and other forms of dementia. This risk increases in tandem with the length of their life expectancy. This pattern is observable in every region of the world. The prevalence of Alzheimer's disease continues to rise with age, as evidenced by the fact that it is now identified in one out of every ten people over the age of 65.

For decades, researchers have been interested in studying the changes in brain function that occur naturally with increasing age. Atrophy is a process that occurs in the brains of elderly people, and it can be observed on every level of biology, from the molecular to the structural. One type of brain atrophy has been connected to elevated blood pressure, which in turn raises the risk of suffering a stroke. Loss of one's capacity to recollect things is the most prevalent type of cognitive deterioration that comes along with aging. Those who experience epileptic convulsions have an increased risk of developing Alzheimer's disease, in comparison to younger people who do not have the condition and who do not show symptoms of epilepsy. This danger is raised to a level that is six times higher.

A person's chronological age is compared to their brain age in Brain AGE, which is the first widely used technique for making such a prediction or evaluation. Brain AGE does this by determining a person's age based on the comparison between their two ages. It accomplishes this by examining the patient's anatomical MRI data in order to ascertain the rate of movement of the patient's brain, which can be either fast or sluggish. The apparatus that is utilized in the recording of electronic brain activity, also referred to as EEG, is both simpler and less costly than the apparatus that is utilized in the recording of magnetic resonance imaging. When it comes to collecting electroencephalograms (EEGs), there are methods that are both non-intrusive and conspicuous accessible. The 10/20 procedure is the one that is utilized the vast majority of the time when getting measurements for an electroencephalogram (EEG). Electrodes are positioned on the forehead of the patient.

The patterns that are generated by the central nervous system are also referred to as brain waves, and they can be captured and analyzed with the help of an electroencephalogram. It is possible to evaluate brain waves in terms of both the physical and chronological dimensions as a result of the fact that brain waves have both an amplitude and a frequency. This makes it possible to track changes in brain activity over time. The different parts of a person's brain do not produce the same wave at the same time, and each individual's pattern of brain waves has its own completely distinctive structure.

It is possible to perform research on how the brain matures by comparing a patient's "biological age," which is calculated using the patient's birth date, to the patient's "brain age," which is calculated using the patient's current age. By investigating the role that recurrent neural networks and enlarged short-term memories play in the development of these conditions, the purpose of this study is to classify and determine the age of the brains of epileptic patients. As a result of the encouraging results that RNNs have obtained with longitudinal data, they are currently the center of a substantial quantity of research. This is because RNNs are a recurrent neural network. Despite the obvious potential that RNNs hold for accomplishing this task, surprisingly little research has been done on the application of RNNs to forecasting mental aging. This is surprising because RNNs have the potential to accomplish this task. The vast majority of studies have been fruitful as a result of the researchers' utilization of traditional machine learning techniques or the implementation of CNN architecture. The EEG Corpus at Temple University is an extensive collection of electroencephalograms (EEG) recordings that have been gathered from a wide variety of individuals over the period of a number of years.

The findings of this investigation into these six versions have already been written up and posted online. The following are the conclusions that are thought to be the most significant of those considered. When the CNN model that was constructed, was evaluated against the Abnormal EEG dataset, it received an MAE value of 8 years of age. This was the result of the evaluation. The BLSTM and BGRU models that we looked into achieve an MAE number that is at least seven years older than the CNN model that is frequently used when it comes to the precision of regression predictions. This is in comparison to the CNN model, which is the model that is most commonly used. Using a categorical analysis, Kaushik et al.

achieved an accuracy of 93.69% when attempting to forecast a person's age; however, the models that were recommended and the dataset that was used achieved an accuracy of 99%. As a direct consequence of the recording procedure, there is a possibility that there will be some crossover between the ensembles. It's possible that this is due to the fact that the DWT method was utilized in the experiments that Kaushik and his colleagues carried out [22]. The discrete wavelet transform (DWT) methodology makes use of an algorithm to divide the total frequency range into several separate regions. Because of this, there is a possibility that there will be some crossover between the regions. The data that were used by Kaushik et al. came from an original source. The researchers themselves were the ones who collected the EEG samples and experimented with a variety of recording intervals and processing approaches. As a result, the data that were used by Kaushik et al. came from an original source.

While finding a perfect model for a particular problem is not possible as the range of possible implementations is so vast, the advantages of the LSTM and GRU architectures cannot be ignored, as they are able to perform well enough in terms of the raw patient EEG data in the regression analysis, reaching MAE values close to and even improved from the benchmark, as well as performing quite well on this particular dataset regarding age classification. On patients' uncontrolled EEG data, the patterns that were used generate outstanding results with only a small degree of signal reduction. This was accomplished with very little signal loss. The discrete wavelet transform and the rapid Fourier transform are just two examples of the signal-preprocessing techniques used by a large number of other academicians in order to determine one of the five EEG frequency bands described above. Discrete wavelet transform and rapid Fourier transform are two more examples of possible approaches. The presented implications, on the other hand, are obtainable from the raw patient data by employing a straightforward bandpass filter in order to retrieve beta brain waves. On the other hand, our method demonstrates that these signal-preprocessing techniques are not essential because they can be acquired straight from the patient data. This was the main finding of our research.

The results of this study are completely predicated on information collected from people who have, at some point in their lives, either recently or in the more distant past, experienced seizures. There is a substantial body of work in this field that makes use of either a database that was individually collected by the author or a database that was made available to the general public. The individuals who have contributed to the information that is available to the public are typically younger and have only been documenting for a constrained period of time. Because the researchers wanted the information gathered from the patients to remain confidential and to be as simple to access as feasible, this portion of the study was skipped. While there are other publicly available EEG databases, such as the Boston Children's Hospital database, they often do not contain the patients' age information, are focused on a subset of younger demographic patients, or contain a very small subset of patient signals that would restrict model efficiency. It is possible that it will be necessary to investigate additional preparatory techniques in order to bring the general quality of the models that are used up to a higher standard. Even though introductory steps have been investigated using FFT and DWT, the results have been disappointing in terms of the work done on raw EEG data and the effectiveness of the LSTM and GRU model designs. This is because the results have shown that the FFT and DWT methods are not able to accurately represent the data. According to the findings of the study carried out, which analyzed the brain waves of 60 patients and divided them into one of six age groups spanning from 6 to 55 years old, beta brain waves were discovered to be the most reliable indicator of age. In light of this, it is possible to generate improved results for age categorization or age projection in individuals who have a history of seizures by considering additional frequency bands or a mixture of those bands. This can be done in order to account for the fact that additional frequency bands can be blended together. There is still much work to be done in terms of the implementation of signal extraction or signal-preprocessing techniques, as well as investigation into the influence these techniques have. However, when endeavoring to anticipate or categorize a patient's age based on the signals in their brain, the utilization of deep learning models in conjunction with the EEG brain signal-processing techniques allowed for the production of appropriate findings. This was possible because of the fact that these techniques allowed for the production of appropriate findings. If the results that are obtained are on pace with, or even better than, those that its contemporaries have achieved, then it is conceivable that more complex signal processing is not necessary than what is generally anticipated to be the case. This is because all that is necessary to acquire the desired frequency range is a basic band pass filter. This is due to the reality that there is no other method available.

REFERENCES

[1] Mu, R.; Zeng, X. A Review of Deep Learning Research. TIISs 2019, 13, 1738–1764, doi:10.3837/tiis.2019.04.001.

[2] Zhang, L.; Jia, J.; Li, Y.; Gao, W.; Wang, M. Deep Learning based Rapid Diagnosis System for Identifying Tomato Nutrition Disorders, KSII Trans. Internet Inf. Syst. 2019, 13, 2012–2027, doi: 10.3837/tiis.2019.04.015.

[3] Ganapathy, N.; Swaminathan, R.; Deserno, T.M.; Deep learning on 1-D biosignals: a taxonomy-based survey. Yearbook Med. Inf. 2018, 27, 098–109

[4] Zhang, D.; Yao, L.; Chen, K.; Wang, S.; Chang, X.; Liu, Y. Making Sense of Spatio-Temporal Preserving Representations for EEG-Based Human Intention Recognition. IEEE Trans. Cybern. 2019, 1–12, doi: 10.1109/TCYB.2019.2905157.

[5] PubMed, Available online: https://www.ncbi.nlm.nih.gov/pubmed/ (accessed on 31 October 2019).

[6] Faust, O.; Hagiwara, Y.; Hong, T.J.; Lih, O.S.; Acharya, U.R. Deep learning for healthcare applications based on physiological signals: A review. Comput. Methods Programs biomed 2018, 1–13.

[7] Tobore, I.; Li, J.; Yuhang, L.; Al-Handarish, Y.; Abhishek, K.; Zedong, N.; Lei, W. Deep Learning Intervention for Health Care Challenges: Some Biomedical Domain Considerations. JMIR mHealth uHealth 2019, 7, e11966

[8] Baig, M.Z.; Kavkli, M., A Survey on Psycho-Physiological Analysis & Measurement Methods in Multimodal Systems. Multimodal Technol. Interact 2019, 3, 37; doi:10.3390/mti3020037.

[9] Yu, Y.; Chen, X.; Cao, S.; Zhang, X.; Chen, X. Exploration of Chinese Sign Language Recognition Using Wearable Sensors Based on Deep Belief Net. IEEE J Biomed Health Inf. 2019, 1–1.

[10] Hu, Y.; Wong, Y.; Wei, W.; Du, Y.; Kankanhalli, M.; Geng, W. A novel attention-based hybrid CNN-RNN architecture for sEMG-based gesture recognition. PloS One

2018, doi: 10.1371/ournal.pone.0206049.

[11] Wei, W.; Dai, Q.; Wong, Y.; Hu, Y.; Kankanhalli, M.; Geng, W. Surface Electromyography-based Gesture Recognition by Multi-view Deep Learning. IEEE Trans. Biomed. Eng. 2019, 66, 2964–2973.

[12] Cote-Allard, U.; Fall, C.L.; Drouin, A.; Campeau-Lecours, A.; Gosselin, C.; Glette, K.; Laviolette, F.; Gosselin, B. Deep learning for electromyographic hand gesture signal classification using transfer learning. IEEE Trans. Neural Syst. Rehabil. Eng. 2019, 27, 760–771.

[13] Sun, W.; Liu, H.; Tang, R.; Lang, Y.; He, J.; Huang, Q. sEMG-Based Hand-Gesture Classification Using a Generative Flow Model. Sensors 2019, 19, 1952, doi:10.3390/s19081952.

[14] Li, C.; Ren, J.; Huang, H.; Wang, B.; Zhu, Y.; Hu, H. PCA and deep learning based myoelectric grasping control of a prosthetic hand. Biomed. Eng. Online 2018, 17, 107, doi:10.1186/s12938-018-0539-8.

[15] Rehman, M.Z.; Waris, A.; Gilani, S.O.; Jochumsen, M.; Niazi, I.K.; Jamil, M.; Farina, D.; Kamavuako, E.N. Multiday EMG-based classification of hand motions with deep learning techniques. Sensors 2018, 18, 2497, doi:10.3390/s18082497.

[16] Wang, W.; Chen, B.; Xia, P.; Hu, J.; Peng, Y. Sensor Fusion for Myoelectric Control Based on Deep Learning with Recurrent Convolutional Neural Networks. Artif. Organs 2018, 42, E272–E282, doi:10.1111/aor.13153.

[17] Xia, P.; Hu, J.; Peng, Y. EMG-based estimation of limb movement using deep learning with recurrent convolutional neural networks. Artif. Organs 2018, 42, E67–E77, doi:10.1111/aor.13004.

[18] Olsson, A.E.; Sager, P.; Andersson, E.; Bjorkman, A.; Malesevic, N.; Antfolk, C. Extraction of Multi-Labelled Movement Information from the Raw HD-sEMG Image with Time-Domain Depth. Sci. Rep. 2019, 9, 7244, doi:10.1038/s41598-019-43676.

[19] Khowailed, I.A.; Abotabl, A. Neural muscle activation detection: A deep learning approach using surface electromyography. J. Biomech. 2019, 95, 109322.

[20] Rance, L.; Ding, Z.; McGregor, A.H.; Bull, A.M.J. Deep learning for musculoskeletal force prediction. Ann. Biomed. Eng. 2019, 47, 778–789, doi:10.1007/s10439-018-02190-0.

[21] Dantas, H.; Warren, D.J.; Wendelken, S.M.; Davis, T.S.; Clark, G.A.; Mathews, V.J. Deep Learning Movement Intent Decoders Trained with Dataset Aggregation for Prosthetic Limb Control. IEEE Trans. Biomed. Eng. 2019, 66, 3192–3203.

[22] Ameri, A.; Akhaee, M.A.; Scheme, E.; Englehart, K. Real-time, simultaneous myoelectric control using a convolutional neural network. PloS One 2018, 13, e0203835, doi: 10.1371/journal.pone.0203835.

[23] Nodera, H.; Osaki, Y.; Yamazaki, H.; Mori, A.; Izumi, Y.; Kaji, R. Deep learning for waveform identification of resting needle electromyography signals. Clin. Neurophysiology 2019, 130, 617–623.

[24] Ribeiro, A.L.P.; Paixao, G.M.M.; Gomes, P.R.; Ribeiro, M.H.; Ribeiro, A.H.; Canazart, J.A.; Oliveira, D.M.; Ferreira, M.P.; Lima, E.M.; Moraes, J.L.; Castro, N.; Ribeiro, L.B.; Macfarlane, P.W. Tele-electrocardiography and bigdata: The CODE (Clinical Outcomes in Digital Electrocardiography) study. J. Electrocardiology 2019, 57, S75-S78.

[25] Cano-Espinosa, C.; Gonzalez, G.; Washko, G.R.; Cazorla, M.; Estepar, R.S.J. Automated Agatston score computation in non-ECG gated CT scans using deep learning. In Proceedings of the Medical Imaging 2018: Image Processing, Texas, United States, 2 March 2018, doi:10.1117/12.2293681.

[26] Chauhan, S.; Vig, L.; Ahmad, S. ECG anomaly class identification using LSTM and error profile modeling. Comput. Biol. Med. 2019, 109, 14–21, doi: 10.1016/j.compbiomed.2019.04.009.

[27] Xia, Y.; Wulan, N.; Wang, K.; Zhang, H. Detecting atrial fibrillation by deep convolutional neural networks. Comput. Biol. Med. 2018, 93, 84–92, doi: 10.1016/j.compbiomed.2017.12.007.

[28] Tan, J.H; Hagiwara, Y.; Pang, W.; Lim, I.; Oh, S.L.; Adam, M.; Tan, R.S.; Chen, M.;

Acharya, U.R. Application of stacked convolutional and long short-term memory network for accurate identification of CAD ECG signals. Comput. Biol. Med. 2018, 94, 19–26, doi: 10.1016/j.compbiomed.2017.12.023.

[29] Smith, S.W.; Walsh, B.; Grauer, K.; Wang, K.; Rapin, J.; Li, J.; Fennell, W.; Taboulet, P. A deep neural network learning algorithm outperforms a conventional algorithm for emergency department electrocardiogram interpretation. J. Electrocardiology 2019, 52, 88–95, doi: 10.1016/j.jelectrocard. 2018.11.013.

[30] Wang, L.; Zhou, X. Detection of congestive heart failure based on LSTM-based deep network via short- term RR intervals.Sensors 2019, 19, 1502, doi:10.3390/s19071502.

[31] Attia, Z.I.; Sugrue, A.; Asirvatham, S.J.; Acherman, M.J.; Kapa, S.; Freidman, P.A.; Noseworthy, P.A. Noninvasive assessment of dofetilide plasma concentration using a deep learning (neural network) analysis of the surface electrocardiogram: A proof of concept study. PloS One 2018, 13, doi: 10.1371/journal.pone.0201059.

[32] S. Siuly, Y. Li, and Y. Zhang, EEG Signal Analysis and Classification. Cham: Springer International Publishing, 2016.

[33] S. Vanneste, J. Song, D. D. Ridder, Thalamocortical dysrhythmia detected by machine learning, NATURE COMMUNICATIONS 9:1103, 2018.

[34] Shoeb, J Guttag, Application of Machine Learning To Epileptic Seizure Detection. Appearing in Proceedings of the 27th International Conference on Machine Learning, Haifa, Israel, 2010.

[35] M. McCarthy, B. Nugent, and K. Lenz, Neuroimmunology and neuroepigenetics in the establishment of sex differences in the brain. Nat Rev Neurosci 18, 471–484, 2017.

[36] Arns, M. et al. EEG alpha asymmetry as a gender-specific predictor of outcome to acute treatment with different antidepressant medications in the randomized iSPOT-D study. Clin. Neurophysiol. 127, 509–519, 2016.

[37] S. Siuly, Y. Li, and Y. Zhang, EEG Signal Analysis and Classification. Cham: Springer International Publishing, 2016.

[38] S. Vanneste, J. Song, D. D. Ridder, Thalamocortical dysrhythmia detected by machine learning, NATURE COMMUNICATIONS 9:1103, 2018.

[39] A. Shoeb, J Guttag, Application of Machine Learning To Epileptic Seizure Detection. Appearing in Proceedings of the 27th International Conference on Machine Learning, Haifa, Israel, 2010.

[40] L. Cahill, Why sex matters for neuroscience. Nat Rev Neurosci, vol. 7, no. 6, pp. 477–484, Jun. 2006.

[41] M. McCarthy, B. Nugent, and K. Lenz, Neuroimmunology and neuroepigenetics in the establishment of sex differences in the brain. Nat Rev Neurosci 18, 471–484, 2017.

[42] Arns, M. et al. EEG alpha asymmetry as a gender-specific predictor of outcome to acute treatment with different antidepressant medications in the randomized iSPOT-D study. Clin. Neurophysiol. 127, 509–519, 2016.

[43] A. R. Clarke, R. J. Barry, R. McCarthy and M. Selikowitz, Age and sex effects in the EEG: development of the normal child, Clinical Neurophysiology Volume 112, Issue 5, Pages 806-814, May 2001.

[44] R. J. Davidson, G. E. Schwartz, E. Pugash and E. Bromfield, Sex differences in patterns of EEG asymmetry, Biological Psychology Volume 4, Issue 2, Pages 119-137, June 1976.

[45] Carrier, J., Land, S., Buysse, D.J., Kupfer, D.J. and Monk, T.H., The effects of age and gender on sleep EEG power spectral density in the middle years of life (ages 20–60 years old). Psychophysiology, 38: 232- 242. 2003.

[46] M. J. A. M. van Putten, S. Olbrich, and M. Arns, Predicting sex from brain rhythms with deep learning, Sci Rep, vol. 8, no. 1, p. 3069, Dec. 2018.

[47] B. Kaur, D. Singh, and P. P. Roy, Age and gender classification using braincomputer interface, Neural Comput & Applic, vol. 31, no. 10, pp. 58875900, Oct. 2019.

[48] Fabien Lotte, Laurent Bougrain, Andrzej Cichocki, Maureen Clerc, Marco Congedo, et al.. A Review of Classification Algorithms for EEGbased Brain-Computer

Interfaces: A 10-year Update. Journal of Neural Engineering, IOP Publishing, 15 (3), pp.55, 2018.

[49] Benjamin Blankertz, Ryota Tomioka, Steven Lemm, Motoaki Kawanabe, Klaus-Robert Muller. Optimizing Spatial Filters for Robust EEG Single- ¨ Trial Analysis. IEEE Signal Processing Magazine 25(1), 41-56, 2008.

[50] Younghak Shin, Seungchan Lee, Minkyu Ahn, Hohyun Cho, Sung Chan Jun, Heung-No Lee, Noise robustness analysis of sparse representation-based classification method for non-stationary EEG signal classification, Biomedical Signal Processing and Control, Volume 21, Pages 8-18, 2015.

[51] Divya Acharya, Anosh Billimoria, Neishka Srivastava, Shivani Goel, and Arpit Bhardwaj. Emotion recognition using fourier transform and genetic programming. Applied Acoustics, 164:107260, 2020.

[52] Divya Acharya, Shivani Goel, Rishi Asthana, and Arpit Bhardwaj. A novel fitness function in genetic programming to handle unbalanced emotion recognition data. Pattern Recognition Letters, 2020.

[53] Samuel Albanie, Arsha Nagrani, Andrea Vedaldi, and Andrew Zisserman. Emotion recognition in speech using cross-modal transfer in the wild. arXiv preprint arXiv:1808.05561, 2018.

[54] Teodiano Freire Bastos-Filho, Andre Ferreira, Ani- ´ bal Cotrina Atencio, Sridhar Arjunan, and Dinesh Kumar. Evaluation of feature extraction techniques in emotional state recognition. In 2012 4th International conference on intelligent human computer interaction (IHCI), pages 1–6. IEEE, 2012.

[55] Arpit Bhardwaj, Aruna Tiwari, M Vishaal Varma, and M Ramesh Krishna. Classification of eeg signals using a novel genetic programming approach. In Proceedings of the Companion Publication of the 2014 Annual Conference on Genetic and Evolutionary Computation, pages 1297–1304, 2014.

[56] Arpit Bhardwaj, Aruna Tiwari, M Vishaal Varma, and M Ramesh Krishna. An analysis of integration of hill climbing in crossover and mutation operation for eeg signal

classification. In Proceedings of the 2015 Annual Conference on Genetic and Evolutionary Computation, pages 209–216. ACM, 2015.

[57] Harshit Bhardwaj, Aditi Sakalle, Arpit Bhardwaj, and Aruna Tiwari. Classification of electroencephalogram signal for the detection of epilepsy using innovative genetic programming. Expert Systems, 36(1):e12338, 2019.

[58] Adnan Mehmood Bhatti, Muhammad Majid, Syed Muhammad Anwar, and Bilal Khan. Human emotion recognition and analysis in response to audio music using brain signals. Computers in Human Behavior, 65:267–275, 2016.

[59] Margaret M Bradley and Peter J Lang. Measuring emotion: the self-assessment manikin and the semantic differential. Journal of behavior therapy and experimental psychiatry, 25(1):49–59, 1994.

[60] Sibnath Deb, Esben Strodl, and Jiandong Sun. Academic stress, parental pressure, anxiety and mental health among indian high school students. International Journal of Psychology and Behavioral Sciences, 5(1):26–34, 2015.

[61] Sander Koelstra, Ashkan Yazdani, Christian Soleymani, Mohammad and, Jong-Seok Lee, Anton Nijholt, Thierry Pun, Touradj Ebrahimi, and Ioannis Patras. Single trial classification of eeg and peripheral physiological signals for recognition of emotions induced by music videos. In International Conference on Brain Informatics, pages 89–100, 2010.

[62] Sander Koelstra, Christian Muhl, Mohammad Soleymani, Jong-Seok Lee, Ashkan Yazdani, Touradj Ebrahimi, Thierry Pun, Anton Nijholt, and Ioannis Patras. Deap: A database for emotion analysis; using physiological signals. IEEE transactions on affective computing, 3(1): 18–31, 2011.

[63] Yuan-Pin Lin, Chi-Hong Wang, Tzyy-Ping Jung, TienLin Wu, Shyh-Kang Jeng, Jeng-Ren Duann, and JyhHorng Chen. Eeg-based emotion recognition in music listening. IEEE Transactions on Biomedical Engineering, 57(7):1798–1806, 2010.

[64] Mufti Mahmud, M Shamim Kaiser, and Amir Hussain. Deep learning in mining biological data, 2020.

[65] AV Medvedev, GI Agoureeva, and AM Murro. A long short-term memory neural network for the detection of epileptiform spikes and high frequency oscillations. Scientific Reports, 9(1):1–10, 2019.

[66] Michael James Scott, Sharath Chandra Guntuku, Yang Huan, Weisi Lin, and Gheorghita Ghinea. Modelling human factors in perceptual multimedia quality: On the role of personality and culture. In Proceedings of the 23rd ACM international conference on Multimedia, pages 481–490. ACM, 2015.